AD-A181 185 VIBRATIONAL MECHANICAL AND THERMAL PROPERTIES OF III-V 1/1
SEMICONDUCTORS(U) NOTRE DAME UNIV IN DEPT OF PHYSICS
J D DOW 20 APR 87 AFOSR-TR-87-0718 AFOSR-85-0331
UNCLASSIFIED F/G 9/1 NL

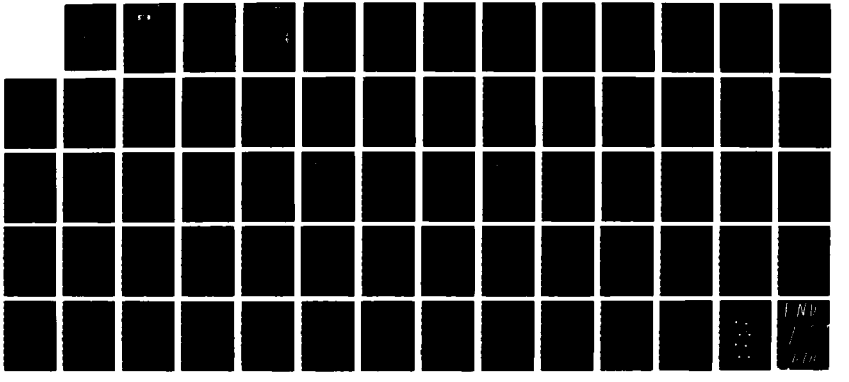

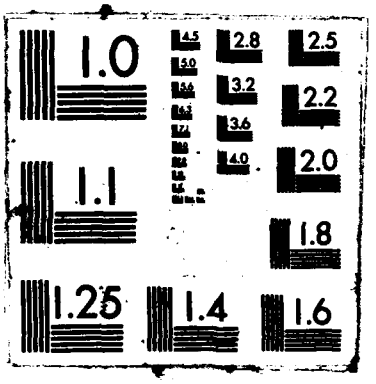
1.0
1.1
1.25
1.4
1.6
1.8
2.0
2.2
2.5
2.8
3.2
3.6
4.0
4.5
5.0

DTIC FILE COPY

(2)

SECURITY CLA

AD-A181 185

REPORT DOCUMENTATION PAGE

1a. REPORT SECURITY CLASSIFICATION: Unclassified	1b. RESTRICTIVE MARKINGS
2a. SECURITY CLASSIFICATION AUTHORITY	3. DISTRIBUTION/AVAILABILITY OF REPORT: Approved for public release; Distribution Unlimited
2b. DECLASSIFICATION/DOWNGRADING SCHEDULE	
4. PERFORMING ORGANIZATION REPORT NUMBER(S)	5. MONITORING ORGANIZATION REPORT NUMBER(S): AFOSR-TR- 87-0718
6a. NAME OF PERFORMING ORGANIZATION: University of Notre Dame	6b. OFFICE SYMBOL (If applicable): D
6c. ADDRESS (City, State and ZIP Code): Notre Dame, IN 46556	7a. NAME OF MONITORING ORGANIZATION: AFOSR
	7b. ADDRESS (City, State and ZIP Code): Bldg 410 Bolling AFB DC 20332-6448
8a. NAME OF FUNDING/SPONSORING ORGANIZATION: AFOSR	8b. OFFICE SYMBOL (If applicable): NE
	9. PROCUREMENT INSTRUMENT IDENTIFICATION NUMBER: AFOSR-85-0331
8c. ADDRESS (City, State and ZIP Code): Bld 410 Bolling Air Force Base, DC 20332	10. SOURCE OF FUNDING NOS.

PROGRAM ELEMENT NO.	PROJECT NO.	TASK NO.	WORK UNIT NO.
61102F	2306	B1	

11. TITLE (Include Security Classification): Vibrational, Mechanical and Thermal Properties of III-V Semiconductors

12. PERSONAL AUTHOR(S): John D. Dow

13a. TYPE OF REPORT	13b. TIME COVERED	14. DATE OF REPORT (Yr., Mo., Day)	15. PAGE COUNT
Annual	FROM 8/15/85 TO 8/14/86	April 20, 1987	65

16. SUPPLEMENTARY NOTATION

17. COSATI CODES			18. SUBJECT TERMS (Continue on reverse if necessary and identify by block number)
FIELD	GROUP	SUB. GR.	

19. ABSTRACT (Continue on reverse if necessary and identify by block number)

We have pursued three major lines of investigation this year: (1) development of theoretical methods for predicting the relaxations of atoms at III-V surfaces, (2) prediction of the vibrational spectra of random III-V and $Hg_{1-x}Cd_xTe$ alloys, and (3) development of a theory of Raman scattering in correlated and clustered alloys. Among other predictions, we have shown that (1) The reconstruction of (110) zincblende surfaces is inhibited by ionic forces, and so the 29° surface anion relaxation angle of GaAs, which was thought to be common to all zincblende (110) surfaces, decreases significantly with increasing ionicity of the semiconductor. (2) Wurtzite (1010) surfaces, to a reasonable approximation, do not reconstruct. (3) The "clustering mode" observed in $Hg_{1-x}Cd_xTe$ Raman spectra is due to Te atoms surrounded by three Hg atoms and one Cd atom, not to vacancy complexes. (4) The effects of correlations and clustering in the Raman

20. DISTRIBUTION/AVAILABILITY OF ABSTRACT	21. ABSTRACT SECURITY CLASSIFICATION
UNCLASSIFIED/UNLIMITED ☒ SAME AS RPT. ☐ DTIC USERS ☐	Unclassified

22a. NAME OF RESPONSIBLE INDIVIDUAL	22b. TELEPHONE NUMBER (Include Area Code)	22c. OFFICE SYMBOL
Capt Walloy	202-767-4931	NE

DD FORM 1473, 83 APR — EDITION OF 1 JAN 73 IS OBSOLETE.

SECURITY CLASSIFICATION OF THIS PAGE

spectra of alloys can be easily predicted using a theory which combines Ising-Monte Carlo techniques and the recursion method.

ANNUAL TECHNICAL REPORT

to

AIR FORCE OFFICE OF SCIENTIFIC RESEARCH
BOLLING AIR FORCE BASE, D.C. 20332

on

VIBRATIONAL, MECHANICAL, AND THERMAL PROPERTIES OF III-V SEMICONDUCTORS

(AF-AFOSR-85-0331)

For Period

August 15, 1985 to August 14, 1986

Submitted by

Professor John D. Dow
Department of Physics
University of Notre Dame
Notre Dame, Indiana 46556

I. SUMMARY

We have pursued three major lines of investigation this year: (1) development of theoretical methods for predicting the relaxations of atoms at III-V surfaces, (2) prediction of the vibrational spectra of random III-V and $Hg_{1-x}Cd_xTe$ alloys, and (3) development of a theory of Raman scattering in correlated and clustered alloys. Among other predicitons, we have shown that (1) The reconstruction of (110) zincblende surfaces is inhibited by ionic forces, and so the 29^o surface anion relaxation angle of GaAs, which was thought to be common to all zincblende (110) surfaces, decreases significantly with increasing ionicity of the semiconductor. (2) Wurtzite $(10\bar{1}0)$ surfaces, to a reasonable approximation, do not reconstruct. (3) The "clustering mode" observed in $Hg_{1-x}Cd_xTe$ Raman spectra is due to Te atoms surrounded by three Hg atoms and one Cd atom, not to vacancy complexes. (4) The effects of correlations and clustering in the Raman spectra of alloys can be easily predicted using a theory which combines Ising-Monte Carlo techniques and the recursion method.

II. RECURSION THEORY OF RANDOM ALLOYS

We have developed recursion method calculations for treating the electronic and vibrational properties of alloys. In particular, we have predicted the electronic structures of $Pb_{1-x}Sn_xTe$ alloys, and shown that the virtual crystal approximation breaks down for the cation s-levels, but not for most of the other electronically relevant bands [1]. To our knowledge, this is the first theory of this sort for IV-VI alloys, materials with rocksalt crystal structure and direct band gaps at the L-point of the Brillouin zone.

We have applied recursion techniques to the vibrational spectra of $Hg_{1-x}Cd_xTe$ and found that the principal features of the Raman scattering data can be understood, and that formerly mysterious features of the data can be attributed to vibrations of specific clusters in the alloy. For example, Amitharaj et al. discovered a "clustering mode" in $Hg_{0.8}Cd_{0.2}Te$, which they suspected might be related to vacancies. We find that this mode is due to a vibrating Te atom surrounded by three Hg atoms and one Cd atom [2]. This ability to understand the spectra of technologically important alloys should be useful for characterizing the materials, and determining the importance of non-random clustering of the atoms in the alloy.

III. Ising-Monte Carlo Theory

We have developed a theory of lattice vibrations of correlated alloys. The usual assumption one makes in treating an alloy such as $Hg_{1-x}Cd_xTe$ is that the atoms occupy sites randomly. This assumption is rarely valid, but is invariably made for lack of a theory of non-randomness.

Our approach is to assume that extended x-ray absorption fine structure data (EXAFS) that are now available at Notre Dame will provide information on pair correlations in alloys. We have constructed a theory which uses these data to construct all the higher-order correlations using an Ising-Monte Carlo scheme. We adjust the "exchange integral" and "magnetic field" of our Ising model to yield the measured pair correlations, and then predict the higher-order correlations and configurations of the non-random alloy. With these configurations we compute the Raman spectra using the recursion method. This combinations of Ising-Monte Carlo and recursion theories yields what we

believe is the first reliable theory of the vibrational properties of non-random alloys.

IV. SURFACE RELAXATION

In order to better understand the mechanical properties of surfaces, we have developed a theory of surface total energies and minimized the surface energies of zincblende semiconductors with respect to rigid rotational bond relaxations. We find that the anions at the GaAs (110) surface rotate out of the surface through a large angle, as is well-established. We also find that the rotation is considerably smaller for more ionic zincblendes (contrary to the accepted viewpoint), and that the more-ionic wurtzite $(10\bar{1}0)$ surfaces, to a good approximation, do not reconstruct.

V. PUBLICATIONS ENCLOSED WITH THIS REPORT

[1] S. Lee and J. D. Dow. Electronic structure of $Pb_{1-x}Sn_xTe$ semiconductor alloys. Submitted.

[2] Z.-W. Fu and J. D. Dow. "Clustering modes" in the vibrational spectra of $Hg_{1-x}Cd_xTe$ alloys. Submitted.

[3] R. V. Kasowski, M.-H. Tsai, and J. D. Dow. Dependence on ionicity of the (110) surface relaxations of zincblende semiconductors. J. Vac. Sci. Technol., in press.

[4] M.-H. Tsai, R. V. Kasowski, and J. D. Dow. Reconstruction of the non-polar $(10\bar{1}0)$ surface of wurtzite AlN and ZnS. Submitted.

file[dow.manus]Le46e204.RMO 10 April 1987 10:35:44

Electronic structure of $Pb_{1-x}Sn_xTe$ semiconductor alloys

Seongbok Lee and John D. Dow

Department of Physics, University of Notre Dame

Notre Dame, Indiana 46556 U.S.A.

(Received [])

The electronic structures of the pseudo-binary alloy semiconductors $Pb_{1-x}Sn_xTe$ are analyzed using a tight-binding model with spin-orbit interaction. The densities of states and the band gaps at the L point are computed for both the effective media using the virtual crystal approximation and the realistic media employing the recursion method, and the results are compared. Both theories exhibit alloying effects such as band broadening, energy shifts, and Dimmock's band crossing phenomenon. However, significant deviations from the virtual-crystal approximation are found for the cation-derived s-like deep valence band states.

PACS Numbers: 71.25.Tn

I. Introduction

The narrow-gap IV-VI semiconductor compounds and their pseudo-binary alloys have unique properties. They have on the average five valence electrons per atom, small direct band gaps at the L point, and high static dielectric constants of order 10^3. They often show a variety of anomalous thermodynamic, acoustic, and electronic properties [1][2]. $Pb_{1-x}Sn_xTe$ is an especially interesting semiconductor alloy because the symmetry of valence and conduction band edges of SnTe is reversed compared to PbTe and other IV-VI semiconductors: The conduction and the valence band edges have L_6^- and L_6^+ symmetry respectively in PbTe and most other IV-VI semiconductors, while the ordering is "Dimmock reversed" in SnTe [1][2][3]. This has an interesting consequence: that the fundamental band gap closes to zero at an intermediate composition x in $Pb_{1-x}Sn_xTe$ [3]. This property of the fundamental energy band gap vanishing for a selected composition means that alloys with compositions near this composition exhibit small band gaps that satisfy the special needs for infrared sources [4] and detectors [5] in modern technology. Therefore it is very important to understand the effects of alloy disorder on the electronic structures of these technologically important materials.

Recently, Spicer et al. [6] have reported experiments indicating the selective breakdown of the virtual crystal approximation for deep valence bands in $Hg_{1-x}Cd_xTe$ (which is a covalent semiconductor alloy containing "light" (Cd) and "heavy" (Hg) atoms), and have identified that phenomenon as resulting from the Hg 6s atomic levels being significantly below the Cd 5s levels. Also, Haas et al. [7] have obtained similar disorder effects theoretically in $Hg_{1-x}Cd_xTe$ using the coherent-potential approximation. Davis

[8] has also found large deviations from virtual-crystal behavior theoretically in $Pb_{1-x}Sr_xS$ where the cations Pb (configuration $6s^26p^2$) and Sr (configuration $5s^2$) differ so much that an average cation potential is meaningless.

The present work analyzes the effects of alloy disorder on the electronic structures of the random alloys $Pb_{1-x}Sn_xTe$ using the recursion method with a tight-binding model. $Pb_{1-x}Sn_xTe$ is an interesting material for this purpose because its constituent semiconductor compounds PbTe and SnTe have very similar overall electronic structures, except for the Dimmock reversal of the valence and conduction band edges; the alloy contains "light" (Sn) and "heavy" (Pb) cations. Moreover, the electronic band structures of these materials have large spin-orbit splittings, and the fundamental gaps are not at the center of the Brillouin zone, $\vec{k}=\vec{0}$. Indeed, some authors believe that PbTe and SnTe are ionic rather than covalent materials [9]. Therefore the usual criteria [10] for the validity of the virtual crystal approximation may not apply.

In Section II, the tight-binding model for the parent semiconductors PbTe and SnTe is discussed, and the recursion method is outlined. In Section III, the results of the calculations are presented and discussed. Section IV summarizes the conclusions.

II. Calculational Procedures

A. Tight-binding model

It is well known that $Pb_{1-x}Sn_xTe$ forms a single phase pseudo-binary alloy over the entire composition range x, with about 2% of lattice constant change from PbTe to SnTe. Both compounds crystallize in the rocksalt structure with lattice constant 6.443 Å for PbTe and 6.327 Å for SnTe [11] at 300 ^{o}K. The electronic structures of PbTe and SnTe (and other IV-VI compounds) have been extensively investigated theoretically and experimentally [1][2]. A variety of computational techniques such as the relativistic augmented plane wave (APW) method [12][13][14], orthonalized plane wave (OPW) method [15], empirical pseudopotential method [16][17][18][19], and relativistic Green's function or Korringa-Kohn-Rostoker method (KKR) [20] have been used to calculate the electronic band structures of these materials. More recently, a self-consistent relativistic APW calculation for SnTe [21] and first-principles pseudopotential total energy calculation for the ground state properties and electronic structures of PbTe and SnTe [22] have been reported. Although considerable differences may exist concerning some details, such as the parity assignments at the L point [23] and gap structures at critical points (for example, some calculations [13][16][21] showed a "hump structure", i.e., the L point is not a minimum or maximum energy point, but a saddle point in SnTe), the general features of the various band structures mentioned above are quite similar. Concentrating on this point and the fact that the recursion method takes its most convenient form in a tight-binding model, we will use in this work the empirical tight-binding Hamiltonian matrix elements of Lent et al. [24], which are obtained by fitting the eigenvalues of the tight-binding Hamiltonian matrix to the experimental band gap at the L point and to band energies at symmetry points, as calculated by Herman et al. [15].

Since the relativistic corrections to the energies of heavy materials, particularly those including Pb, are significant [25][26], the Hamiltonian used for band calculations should include these effects. The relativistic Hamiltonian which produces the energy band structure has the following form [12]

$$H = (p^2/2m) + V + H_{so} + \hbar^2\nabla^2 V/8m^2c^2 - p^4/8m^3c^2 \qquad (1)$$

where V is the periodic crystal potential. The spin-orbit term which may split degenerate levels is

$$H_{so} = \mu\vec{\sigma}\cdot[(\Delta V)\times\vec{p}]/4m^2c^2 \qquad (2)$$

and the remaining terms are the Darwin and mass-velocity terms, respectively.

Employing the ideas of Harrison [27], Chadi [28], and Vogl et al. [29], the nearest-neighbor tight-binding Hamiltonian can be constructed

$$H_0 = \sum_{\vec{R},\sigma,i} [|a,i,\sigma,\vec{R}\rangle E_{i,a} \langle a,i,\sigma,\vec{R}| + |c,i,\sigma,\vec{R}+\vec{d}\rangle E_{i,c} \langle c,i,\sigma,\vec{R}+\vec{d}|]$$

$$+ \sum_{\vec{R},\vec{R}',\sigma,i,j} [|a,i,\sigma,\vec{R}\rangle V_{i,j} \langle c,j,\sigma,\vec{R}'+\vec{d}|$$

$$+ \text{H.c.}] + H_{so} \qquad (3)$$

where H.c. means Hermitian conjugate, $\vec{R}$ are the lattice vectors, i and j are the localized quasi-atomic orbitals for the cation and anion, σ is the spin index (up or down), a and c refer to the anion and cation respectively, and $\vec{d}$

is the position of the cation relative to the anion in any unit cell: $\vec{d} = (a_L/2,0,0)$. The spin-orbit interaction term can be described by the following Hamiltonian

$$H_{so} = \sum_{\vec{R},i,j,\sigma,\sigma'} [|a,i,\sigma,\vec{R}\rangle(\lambda_a/2)\vec{L}_a\cdot\vec{\sigma}_a\langle a,j,\sigma',\vec{R}|$$

$$+|c,i,\sigma,\vec{R}\rangle(\lambda_c/2)\vec{L}_c\cdot\vec{\sigma}_c\langle c,j,\sigma',\vec{R}|] \quad (4)$$

As a basis set, we used eighteen quasi-atomic orbitals localized on each atomic site which are assumed to be mutually orthonormalized by the method of Löwdin [30]: s, p_x, p_y, p_z, $d_{x^2-y^2}$, $d_{3z^2-r^2}$, d_{xy}, d_{yz}, and d_{zx} for each spin up and down state. The parameters of this model are given in Ref. [24], and reproduce the experimental band gaps at the L point [3] (0.186 eV for PbTe and 0.3 eV for SnTe) as well as the calculated band energies of Ref. [15] at the high symmetry points Γ, X, and L. The resulting band structures are given in Ref. [24]. In particular, the Dimmock reversal of the band structure from PbTe to SnTe is correctly reproduced by the model.

B. Recursion method

In a random alloy where the perfect periodicity is lacking, the wave vector $\vec{k}$ is no longer a good quantum number and the simplifications of Bloch's theorem do not apply. Moreover, since the number of possible alloy configurations is infinite, it is necessary to develop a theory that will correctly predict the macroscopic physical properties of an alloy without having to perform ensemble averages of microscopic properties over impossibly

large numbers of alloy configurations. Various approaches have been developed to overcome these difficulties. Among these, effective medium theories such as the virtual crystal approximation (VCA) [31] and the coherent potential approximation (CPA) [6][7][10][32][33][34][35][36] have been commonly used for the study of semiconductor alloys. In this work, we will use the recursion method [8][37] because it does not require any lattice periodicity or effective medium; and, if executed to convergence, does obtain the correct alloy density of states (in contrast with the effective medium models). In this section, we shall briefly present the underlying concept of the recursion method.

For the discussion of electronic structure of disordered systems, the local density of states (LDOS) is a well-defined and useful quantity; it can be written

$$n(E,\vec{r}) = \sum_n |\psi_n(\vec{r})|^2 \, \delta(E-E_n)$$

or

$$= -(1/\pi) \, \mathrm{Im} \, G(\vec{r},\vec{r},E), \qquad (5)$$

where

$$G(\vec{r},\vec{r}',E) = \lim_{\epsilon \to 0} \langle \vec{r} | (E-H+i\epsilon)^{-1} | \vec{r}' \rangle \qquad (6)$$

is the Green's function, and $\psi_n(\vec{r})$ is an eigenfunction of the disordered system with eigenvalue E_n.

We choose as a basis set the localized atomic orbitals centered on the various atoms of a finite cluster, $\phi_m(\vec{r}-\vec{R})$, where m runs over the s, p, and d states. These are orthonormalized Löwdin orbitals [30] and $\vec{R}$ is the atomic site. Now we relabel them as $|i\rangle$ (i=0, 1, 2, ..., N, where N+1 is the total number of orbitals), and take as $|0\rangle$ the particular orbital (either s, p, or d) on the particular atomic site (either anion or cation) we are interested in. In this basis, the local density of states of the state $|0\rangle$ becomes

$$n_0(E) = -(1/\pi)\ \mathrm{Im}\ G_{0,0}(E) \qquad (7)$$

where we define

$$G_{i,j}(\epsilon) = \lim_{\epsilon \to 0} \langle i|(E-H+i\epsilon)^{-1}|j\rangle \qquad (8)$$

When we know the exact eigenvalues and eigenstates, we can calculate the local density of states by the use of equation (5). In actual calculations for realistic models of disordered systems, this approach requires computations that are complicated and often impractical. Other approaches (e.g., the method of moments or the recursion method) are needed to predict the (local) density of states without directly calculating the eigenvalues and eigenvectors.

The recursion method is one such scheme, and uses an analytic expression to obtain the density of states. Since any Hermitian matrix can be transformed into a real symmetric tridiagonal matrix by unitary transformation, the Hamiltonian matrix elements in the new transformed basis $|\nu\rangle$ (ν=0, 1, ..., N) can be written

$$(\mu|H|\nu) = \begin{cases} a_\mu & \nu-\mu \\ b_{\mu+1} & \nu-\mu+1 \\ b_\mu & \nu-\mu-1 \\ 0 & \text{otherwise} \end{cases} \qquad (9)$$

In other words, we have the following recursion equation

$$H|\nu) = b_\nu|\nu-1) + a_\nu|\nu) + b_{\nu+1}|\nu+1) \qquad (10)$$

At the initial iteration, we choose $|0)=|0\rangle$, and set $b_0=0$. Then all the recursion coefficients a_ν and b_ν ($\nu=0, 1, \ldots, N$) can be determined by recursive use of equation (10).

Given the tridiagonalized Hamiltonian (equation (9)), the Green's function can be expressed as a continued-fraction

$$G_{0,0}(E) = \cfrac{1}{E - a_0 - \cfrac{b_1^2}{E - a_1 - \cfrac{b_2^2}{E - a_2 - \cdots}}} \qquad (11)$$

where E has an infinitesimal positive imaginary part. In principle, $G_{0,0}(E)$ can be determined as exactly as possible by expanding it to the N-th level. However, in practice the expansion is cut off at some finite level L, and the remainder is neglected here.

As a final step, the continued-fraction form of Green's function is decomposed into partial fractions and the imaginary part is taken to obtain the local density of states. Thus the local density of states is expressed as a sum of Dirac delta functions, and a relatively accurate integrated local density of states is evaluated by integration. Then the local density of states itself is determined by numerical differentiation. Details of the method can be found in Ref. [37]; computer programs for executing the recursion method are available [38].

Since we are interested in the macroscopic properties of the alloy, the local density of states should be averaged over all sites in the alloy. This can be done by the usual method, i.e., finding the local densities of states for each site and taking the average of them. However, it is an extremely time-consuming procedure for a large cluster. In practice, it is better to choose an initial state $|0\rangle$ that is a sum over either all cation or anion sites of $\phi_m(\vec{r}-\vec{R})$ with m the same for each site and with random signs on the various sites. Then the off-diagonal terms $\langle n|G|m\rangle$ that enter equation (7) approximately cancel out, due to the random signs, giving a reasonable site average for the large cluster.

III. Results and Discussion

We first calculate the density of states for the perfect crystals PbTe and SnTe employing the nearest-neighbor tight-binding model discussed in the previous section. The results are shown in Figs. (1) and (2). The dot-dashed curve is the density of states obtained by the Lehmann-Taut method [39]. In this method, the Brillouin zone is decomposed into a set of tetrahedra, and

the integration over the Brillouin zone is evaluated using an analytic expression. The solid curve is from the recursion method. A 12x12x12 atom cluster was generated to simulate the perfect infinite crystal, and the local density of states for each orbital was calculated with the initial state $|0\rangle=|0\rangle$ being a linear superposition of $\phi_m(\vec{r}-\vec{R})$ from all the sites on a given sublattice, with random signs (±) on each site. Periodic boundary conditions were used, and the recursion was iterated to L=51 levels -- that is, the continued-fraction expansion of the Green's function was cut off at the L=51 level. Then all the local densities of states were summed to give the (global) density of states.

The overall agreement between the two methods is very good, except for some minor details such as the peak structures and the band gap smearing; the differences between the results of the recursion method and the Lehmann-Taut method are within the tolerable range. The δ-function-like peaks are associated with van Hove singularities [40] due to the long-range order. The more or less smooth peaks in the upper valence bands given by the recursion method (solid curve) are partly due to the finite size of the cluster and partly due to the limited resolution of the present method because of the finite cutoff at L=51. (We determined this by varying the size of the cluster and L.) Another difference is that while the Lehmann-Taut method clearly shows the band gap to contain no states, the band edges are smeared in the recursion method. The main reasons for this are the limited resolution of the method and the incomplete cancellation of the off-diagonal elements of the Green's function due to the choice of randomly phased initial state. The band edges can be sharpened by choosing the initial state on the center of a cluster or by investigating the spectral density of states as will be discussed later. In

Fig. (3), the contribution of each orbital to the density of states of PbTe is displayed. The lowest valence band is predominantly anion s-like, and the middle valence band is cation s-like. The upper valence bands have dominant anion p-like character, while the lower conduction bands are p-like and cation derived. This can be visualized by the following simple picture. The Pb atom has four valence electrons ($6s^2 6p^2$) with free-atomic orbital energies -12.42 eV and -6.95 eV (relative to vacuum) for s- and p- orbitals respectively, and the Te atom has six valence electrons ($5s^2 5p^4$) with orbital energies -19.05 eV (5s) and -9.79 eV (5p) [41]. The two 5s electrons of Te, which have the lowest orbital energies, form an isolated valence band deep in energy, and the two 6s electrons of Pb form a middle valence band. The two 6p electrons of Pb and the four 5p electrons of Te interact with each other to form bonding (valence band) and antibonding (conduction band) bands. Therefore, alloying PbTe and SnTe, which is equivalent to distributing Pb and Sn atoms randomly on cation sites, has the largest effect on the cation-like middle valence band. The characteristics of the local density of states structure in SnTe is similar to that of PbTe (see Fig. (4)) the 5s and 5p free-atomic orbital energies of Sn are at -12.97 eV and -7.21 eV, respectively.

We generate a model of the random alloy $Pb_{1-x}Sn_xTe$ by randomly occupying cation sites by either Pb (with probability 1-x) or Sn (with probability x), while all anion sites are occupied by Te. The matrix elements of the alloy Hamiltonian are derived from those of PbTe and SnTe as follows: On cation sites, we use either PbTe or SnTe matrix elements, depending on whether the site was occupied by Pb or Sn. On Te sites, we average the PbTe and SnTe matrix elements, weighting the average in proportion to the number of neighboring Pb and Sn atoms to the Te. Then the densities of states for

$Pb_{1-x}Sn_xTe$ are calculated using both the virtual crystal approximation and the recursion method for a number of compositions x. Again, the density of states is obtained by the use of the Lehmann-Taut method in the virtual crystal approximation, and a 12x12x12 atom cluster is used in the recursion method with periodic boundary conditions. In order to avoid sample dependent results, we repeated the calculations for five different alloy configurations of 12^3 atoms, and averaged the densities of states. The results are shown in Figs. (5), (6), (7), and (8). The solid curves represent the recursion density of states, and the dot-dashed curves are for the virtual crystal approximation (VCA) results. Both the virtual crystal approximation and the recursion density of states show the alloying effects i.e., energy shifts and width changes of the density of states peaks. However, analysis of the middle valence band near -7 eV, which has the greatest alloying effects, clearly reveals the differences between the predictions of the two methods -- the effects of disorder. This band is a doublet, with its low- and high-energy components due to Pb and Sn s-states, respectively.

Fortunately the results we find agree rather well with what is expected, based on the Onodera-Toyozawa theory of alloys [10] -- despite the fact that that theory, to our knowledge, has not been applied previously to alloys with fundamental band gaps at the L-point of the Brillouin zone. The density of states spectra of the alloys exhibit some features that are "persistent" and others that are "amalgamated" in the terminology of Ref. [10]. The persistent features are associated with the cation-like middle valence bands: the Pb 6s-like and Sn 5s-like bands that retain their characters in the alloy because the perfect-crystal bands do not overlap in energy. The remaining bands are "amalgamated" and tend to form hybrids of the PbTe and SnTe bands rather than

exhibit separate PbTe- and SnTe-like bands. This amalgamation occurs because the PbTe and SnTe bands overlap in energy, and hence mix in the alloy [10]. Bands that fall within this amalgamated regime can generally be described, in a first approximation, by the virtual crystal approximation.

Although it is straightforward to include a valence band offset in the calculation by adding a constant energy to all of the diagonal matrix elements of either PbTe or SnTe (by construction, the matrix elements of Ref. [24] place the zero of energy at the valence band maximum), we have not done so here because the offset is thought to be small (of order 60 meV) [42], almost negligible on the scale of the figures.

It is well known that the fundamental band gap of $Pb_{1-x}Sn_xTe$ closes at some intermediate composition because of the inverted band structure of SnTe. We calculated $E(L_6^-)-E(L_6^+)$ of $Pb_{1-x}Sn_xTe$ as a function of composition x by diagonalizing the virtual-crystal empirical tight-binding Hamiltonian (closed circles in Fig. (9)). Also the corresponding quantity can be calculated using the recursion method. In alloys, the translational symmetry is broken, thus the wave vector $\vec{k}$ is not a good quantum number. However, we still can define the spectral density functions analogous to the perfect crystal by the following [8]

$$A(\vec{k},E) = -(1/\pi)\lim_{\epsilon\to 0} \mathrm{Im} \langle b,i,\sigma,\vec{k}|G(E+i\epsilon)|b,i,\sigma,\vec{k}\rangle \qquad (12)$$

where $|b,i,\sigma,\vec{k}\rangle$ is a normalized Bloch sum over all unit cells of orbital i with spin σ on each atomic site b (anion or cation). Then the position and broadening of the peak represents the energy shift and damping of a particular

quasiparticle state of energy E and wave vector $\vec{k}$. Since L_6^+ (L_6^-) has anion (cation) p-like character, a Bloch sum of $(p_x+p_y+p_z)/\sqrt{3}$ on each anion (cation) site at the L point is chosen as the initial state $|0\rangle$ for L_6^+ (L_6^-), and the spectral density of states $A(\vec{k},E)$ is calculated. Then the gap is defined by the differences in the peak values of $A(\vec{k},E)$, i.e., $E(L_6^-)-E(L_6^+)$. The theoretical predictions are shown also in Fig. (9) (closed triangles) in comparison with a linear interpolation of the experimental band gaps of PbTe and SnTe [3] (solid line). The theoretical uncertainty in $E(L_6^-)-E(L_6^+)$ is $\sim \pm 0.02$ eV for $0<x<1$. The calculated band gap is almost a linear function of composition x and compares well with the experimental results.

IV. Summary

The electronic structures of $Pb_{1-x}Sn_xTe$ alloys including their parent semiconductor compounds have been analyzed using the tight-binding model with spin-orbit interaction. The densities of states were computed for both the effective media using the virtual crystal approximation and the realistic media employing the recursion method, and the results were compared. As expected, both theories exhibited alloying effects such as band broadening and energy shifts. However, the two methods differed in their predictions for the cation-derived s-like states, which experienced the greatest alloying effect. The alloy composition dependence of the band gap at the L point was analyzed, and exhibits Dimmock's band crossing phenomenon. The above facts show that the recursion method is a useful tool for the study of the electronic structure of random $Pb_{1-x}Sn_xTe$, and in particular for the cation-like middle valence band. However, they also show that the virtual crystal approximation provides a remarkably good description of the electronically important top valence and

bottom conduction bands. Finally, they demonstrate that the Onodera-Toyozawa criteria can be applied to $Pb_{1-x}Sn_xTe$, even though these alloys have their fundamental band gaps at L: the cation-like s-like middle valence bands are "persistent" while the top valence band and lowest conduction band are "amalgamated."

Acknowledgments -- We are grateful to the Office of Naval Research (Contract No. N00014-84-K-0352), the Air Force Office of Scientific Research (Contract No. AFOSR-85-0331), the University of Notre Dame, and the University of Illinois at Urbana-Champaign Physics Department for their support of this work. We benefitted greatly from stimulating conversations with M. Bowen, E. Ho, C. Lent, and O. Sankey.

References

[1] (a) W. Jantsch, in Dynamical Properties of IV-VI Compounds, Springer Tracts in Modern Physics (Springer-Verlag, Berlin, Heidelberg, New York, Tokyo, 1983), Vol. 99, p. 1; (b) A. Bussmann-Holder, H. Bilz, and P. Vogl, ibid. Vol. 99, p. 51

[2] G. Nimtz and B. Schlicht, in Narrow-Gap Semiconductors, Springer Tracts in Modern Physics (Springer-Verlag, Berlin, Heidelberg, New York, Tokyo, 1983), Vol. 98, p. 1

[3] J. O. Dimmock, I. Melngailis, and A. J. Strauss, Phys. Rev. Lett. 16, 1193 (1966).

[4] H. Preier, Appl. Phys. 20, 189 (1979).

[5] H. Holloway, J. Appl. Phys. 50, 1386 (1979).

[6] W. E. Spicer, J. A. Silberman, M. Morgan, I. Lindau, J. A. Wilson, A.-B. Chen, and A. Sher, Phys. Rev. Lett. 49, 948 (1982).

[7] K. C. Hass, H. Ehrenreich, and B. Velicky, Phys. Rev. B27, 1088 (1983).

[8] L. C. Davis, Phys. Rev. B 28, 6961 (1983).

[9] M. Schlüter, G. Martinez, and M. L. Cohen, Phys. Rev. B 11, 3808 (1975).

[10] Y. Onodera and Y. Toyozawa, J. Phys. Soc. Jap. 24, 341 (1968).

[11] R. F. Bis and J. R. Dixon, J. Appl. Phys. 40, 1918 (1969).

[12] J. B. Conklin, L. E. Johnson, and G. W. Pratt, Phys. Rev. 137, A 1282 (1965).

[13] S. Rabii, Phys. Rev. 182, 821 (1969).

[14] S. Rabii and R. H. Lasseter, Phys. Rev. Lett. 33, 703 (1974).

[15] F. Herman, R. L. Kortum, I. B. Ortenberg, and J. P. van Dyke, J. Phys. (Paris) 29, C4-62 (1968).

[16] Y. W. Tung and M. L. Cohen, Phys. Rev. 180, 823 (1969).

[17] R. L. Bernick and L. Kleinman, Solid State Commun. 8, 569 (1970).

[18] S. E. Kohn, P. Y. Yu, Y. Petroff, Y. R. Shen, Y. Tsang, and M. L. Cohen, Phys. Rev. B 8, 1477 (1973).

[19] G. Martinez, M. Schlüter, and M. L. Cohen, Phys. Rev. B 11, 651 (1975).

[20] H. Overhof and U. Rössler, Phys. Stat. Sol. 37, 691 (1970); J. Korringa, Physica 13, 392 (1947); W. Kohn and N. Rostoker, Phys. Rev. 94, 1111 (1954).

[21] J. S. Melvin and D. C. Hendry, J. Phys. C 12, 3003 (1979).

[22] K. M. Rabe and J. D. Joannopoulos, Phys. Rev. B 32, 2302 (1985).

[23] See for example, G. Martinez and M. L. Cohen, Phys. Rev. Lett. 35, 1746 (1975), and references therein.

[24] C. S. Lent, M. A. Bowen, J. D. Dow, R. S. Allgaier, O. F. Sankey, and E. S. Ho, Superlattices and Microstructures 2, 491 (1986).

[25] L. E. Johnson, J. B. Conklin, and G. W. Pratt, Phys. Rev. Lett. 11, 538 (1963).

[26] F. Herman, C. D. Kuglin, K. F. Cuff, and R. L. Kortum, Phys. Rev. Lett. 11, 541 (1963).

[27] W. A. Harrison, Phys. Rev. B 8, 4487 (1973).

[28] D. J. Chadi, Phys. Rev. B 16, 790 (1977).

[29] P. Vogl, H. P. Hjalmarson, and J. D. Dow, J. Phys. Chem. Solids 44, 365 (1983).

[30] P.-O. Löwdin, J. Chem. Phys. 17, 365 (1950).

[31] L. Northeim, Ann. Phys. [5] 9, 607 and 641 (1931); F. Bassani and D. Brust, Phys. Rev. 131, 1524 (1963); H. Amar, K. H. Johnson, and C. B. Sommers, ibid. 153, 655 (1967); M. M. Pant and S. K. Joshi, ibid. 184, 635 (1969).

[32] P. Soven, Phys. Rev. 156, 809 (1967).

[33] D. W. Taylor, Phys. Rev. B15, 1017 (1967).

[34] B. Velicky, S. Kirkpatrick, and H. Ehrenreich, Phys. Rev. 175, 747 (1968).

[35] A.-B. Chen and A. Sher, Phys. Rev. B17, 4726 (1978).

[36] A.-B. Chen and A. Sher, Phys. Rev. B23, 5360 (1981).

[37] R. Haydock, in Solid State Physics, edited by H. Ehrenreich, F. Seitz, and D. Turnbull (Academic, New York, 1980), Vol. 35, p. 215.

[38] S. Lee, Ph.D. thesis, University of Illinois at Urbana-Champaign physics department, 1986, unpublished.

[39] G. Lehmann and M. Taut, Phys. Stat. Sol. (b) 54, 469 (1972).

[40] L. van Hove, Phys. Rev. 89, 1189 (1953).

[41] C. F. Fisher, Atomic Data 4, 301 (1972).

[42] K. E. Ambrosch, H. Clemens, E. J. Fantner, G. Bauer, M. Kriechbaum, P. Kocevar, and R. J. Nicholas, Surface Science, 142, 571 (1984).

FIGURE CAPTIONS

Fig. (1) The virtual crystal approximation (dot-dashed curve) and the recursion method (solid curve) density of states in PbTe. A 12x12x12 atom cluster with periodic boundary conditions was used in the recursion method. The zero of energy is the valence band maximum.

Fig. (2) The virtual crystal approximation (dot-dashed curve) and the recursion method (solid curve) density of states in SnTe. A 12x12x12 atom cluster with periodic boundary conditions was used in the recursion method.

Fig. (3) Local density of states for cation (dot-dashed curve) and anion (solid curve) calculated by the recursion method in PbTe.

Fig. (4) Local density of states for cation (dot-dashed curve) and anion (solid curve) calculated by the recursion method in SnTe.

Fig. (5) The virtual crystal approximation (dot-dashed curve) and the recursion method (solid curve) density of states in $Pb_{0.3}Sn_{0.7}Te$. A 12x12x12 atom cluster with periodic boundary condition was used in the recursion method.

Fig. (6) The virtual crystal approximation (dot-dashed curve) and the recursion method (solid curve) density of states in $Pb_{0.4}Sn_{0.6}Te$. A 12x12x12 atom cluster with periodic boundary condition was used in the recursion method.

Fig. (7) The virtual crystal approximation (dot-dashed curve) and the recursion method (solid curve) density of states in $Pb_{0.5}Sn_{0.5}Te$. A 12x12x12 atom cluster with periodic boundary condition was used in the recursion method.

Fig. (8) The virtual crystal approximation (dot-dashed curve) and the recursion method (solid curve) density of states in $Pb_{0.6}Sn_{0.4}Te$. A 12x12x12 atom cluster with periodic boundary condition was used in the recursion method.

Fig. (9) The band gap $E(L_6^-)$-$E(L_6^+)$ of $Pb_{1-x}Sn_xTe$ versus composition x. The closed circles (triangles) are obtained using the virtual crystal approximation (the recursion method), and the solid line represents the interpolation of PbTe and SnTe experimental results of Ref. [3].

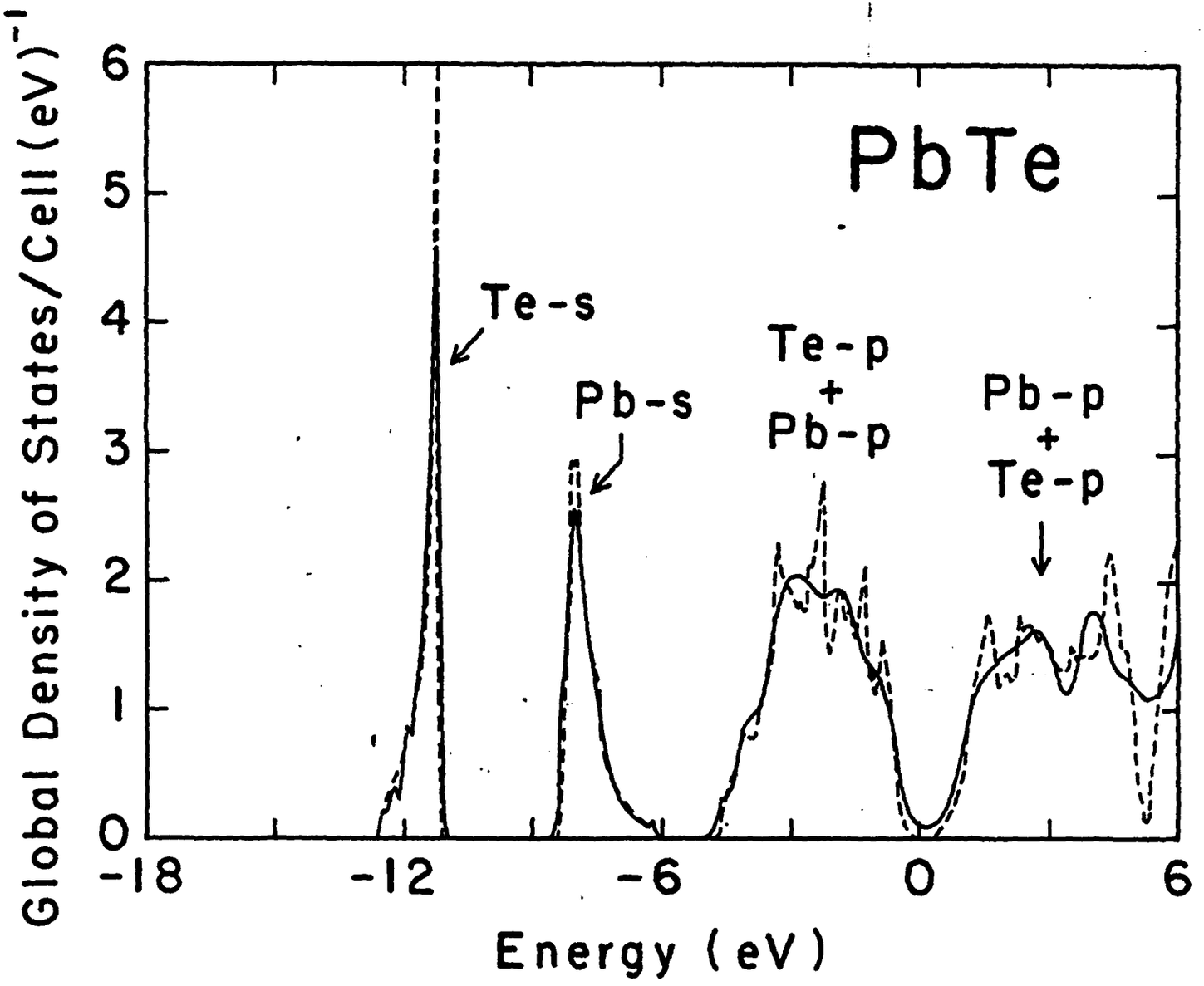
PbTe
Te-s
Pb-s
Te-p
+
Pb-p
Pb-p
+
Te-p
Global Density of States/Cell (eV)$^{-1}$
Energy (eV)
6
5
4
3
2
1
0
-18
-12
-6
0
6

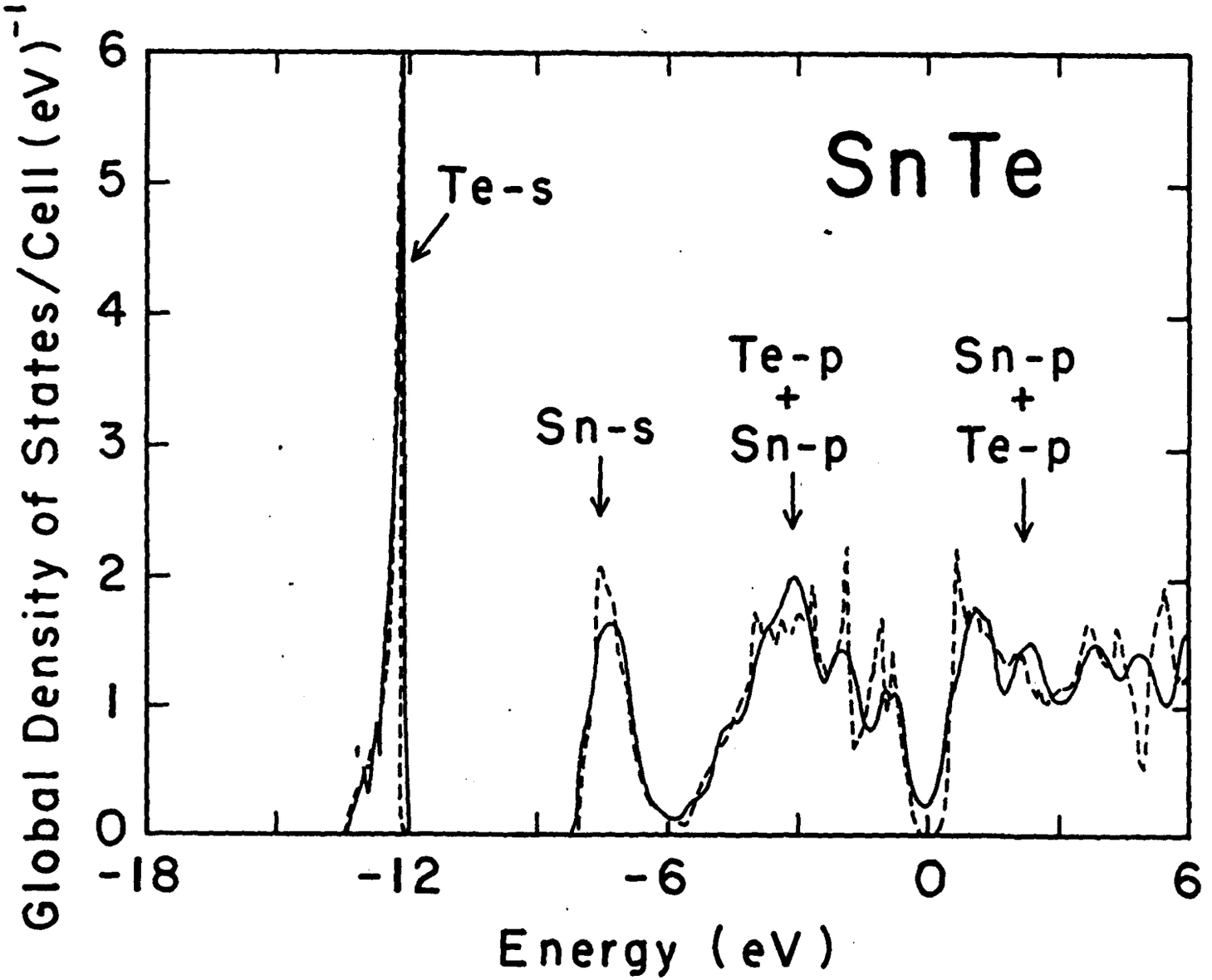
SnTe
Te-s
Sn-s
Te-p
+
Sn-p
Sn-p
+
Te-p
Global Density of States/Cell (eV)$^{-1}$
Energy (eV)
0
1
2
3
4
5
6
-18
-12
-6
0
6

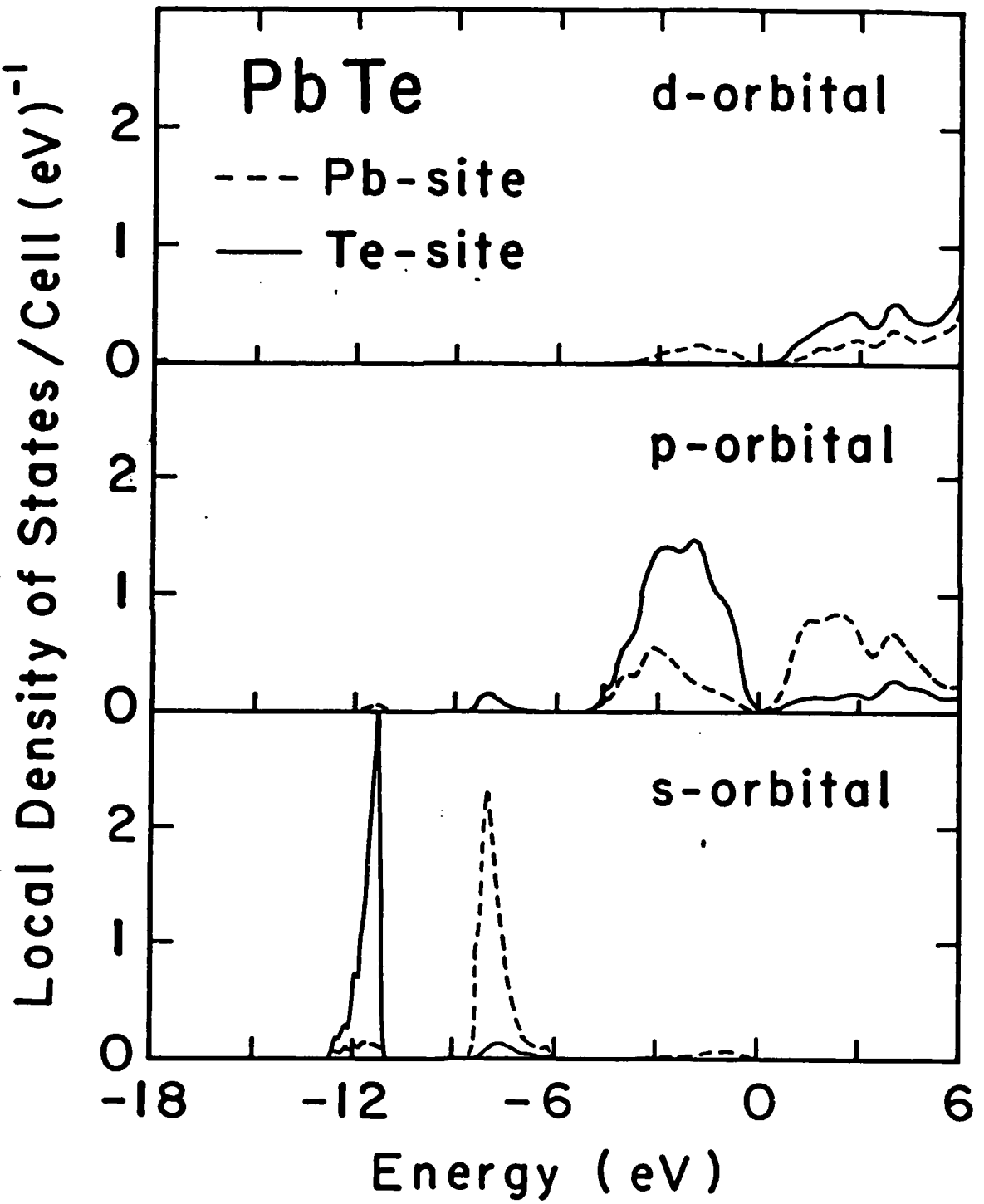
PbTe
d-orbital
Pb-site
Te-site
p-orbital
s-orbital
Local Density of States/Cell (eV)$^{-1}$
0
1
2
-18
-12
-6
0
6
Energy (eV)

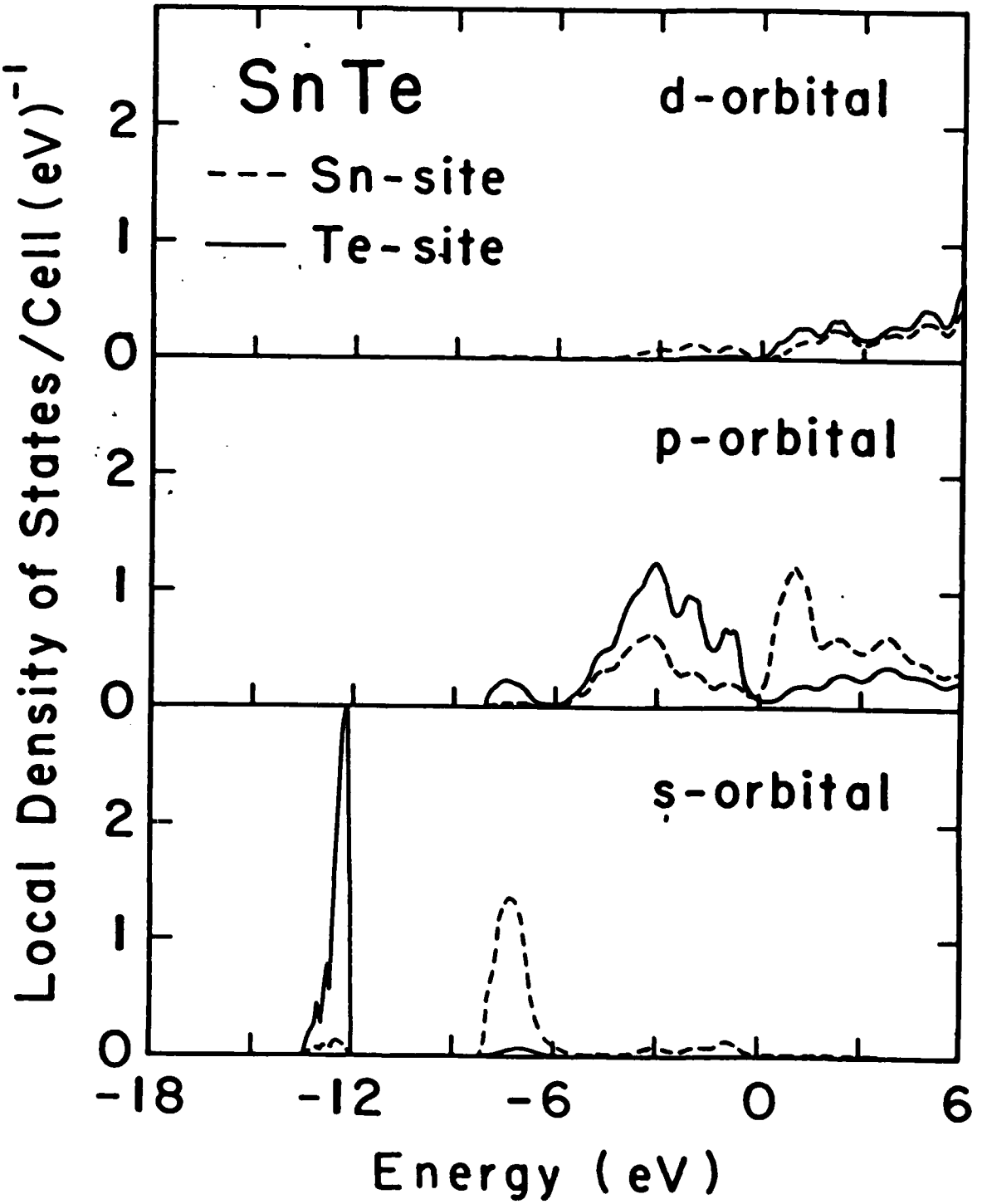
SnTe
d-orbital
--- Sn-site
—— Te-site
p-orbital
s-orbital
Local Density of States/Cell (eV)⁻¹
2
1
0
-18
-12
-6
0
6
Energy (eV)

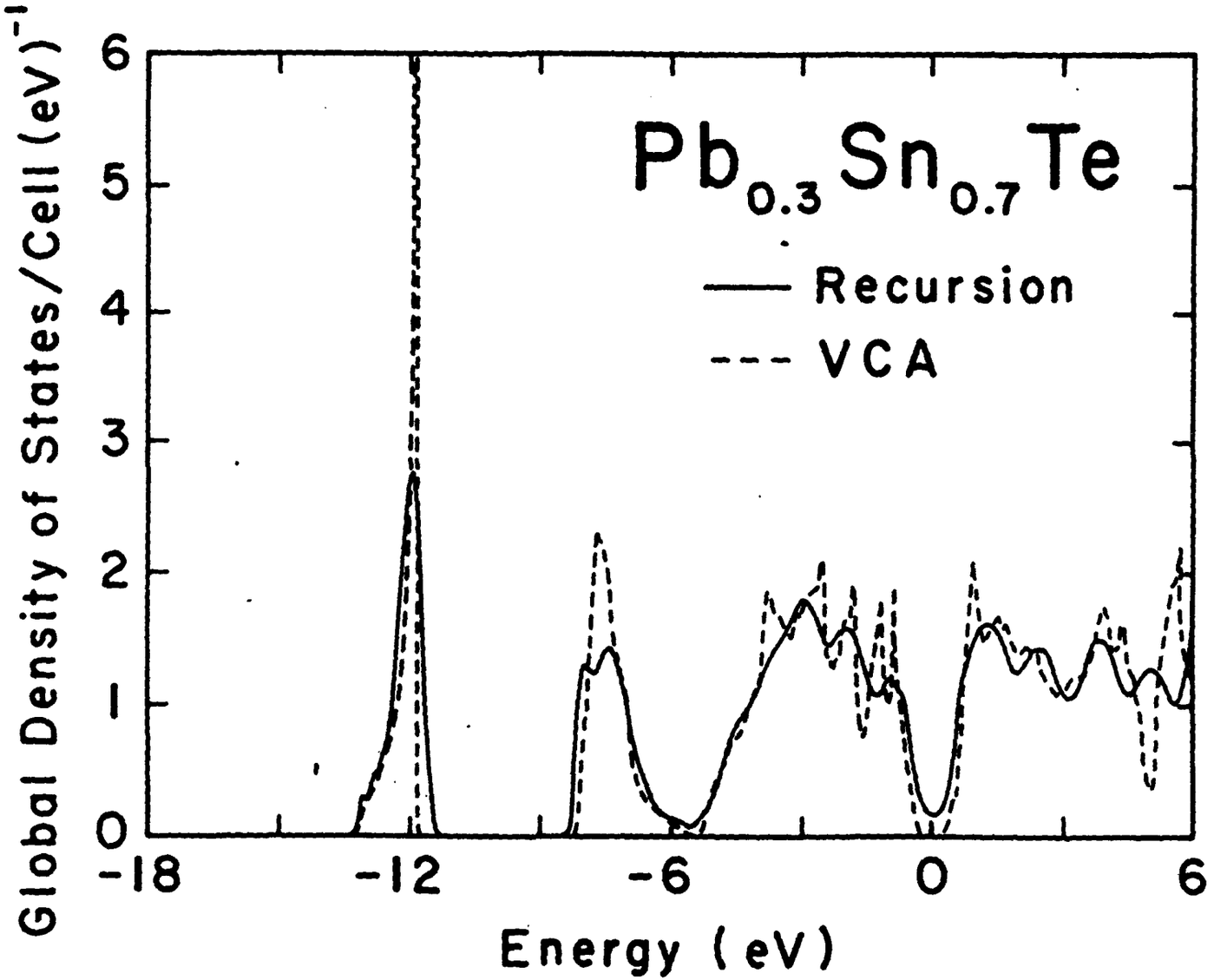
Pb0.3Sn0.7Te
Recursion
VCA
Global Density of States/Cell (eV)-1
Energy (eV)
6
5
4
3
2
1
0
-18
-12
-6
0
6

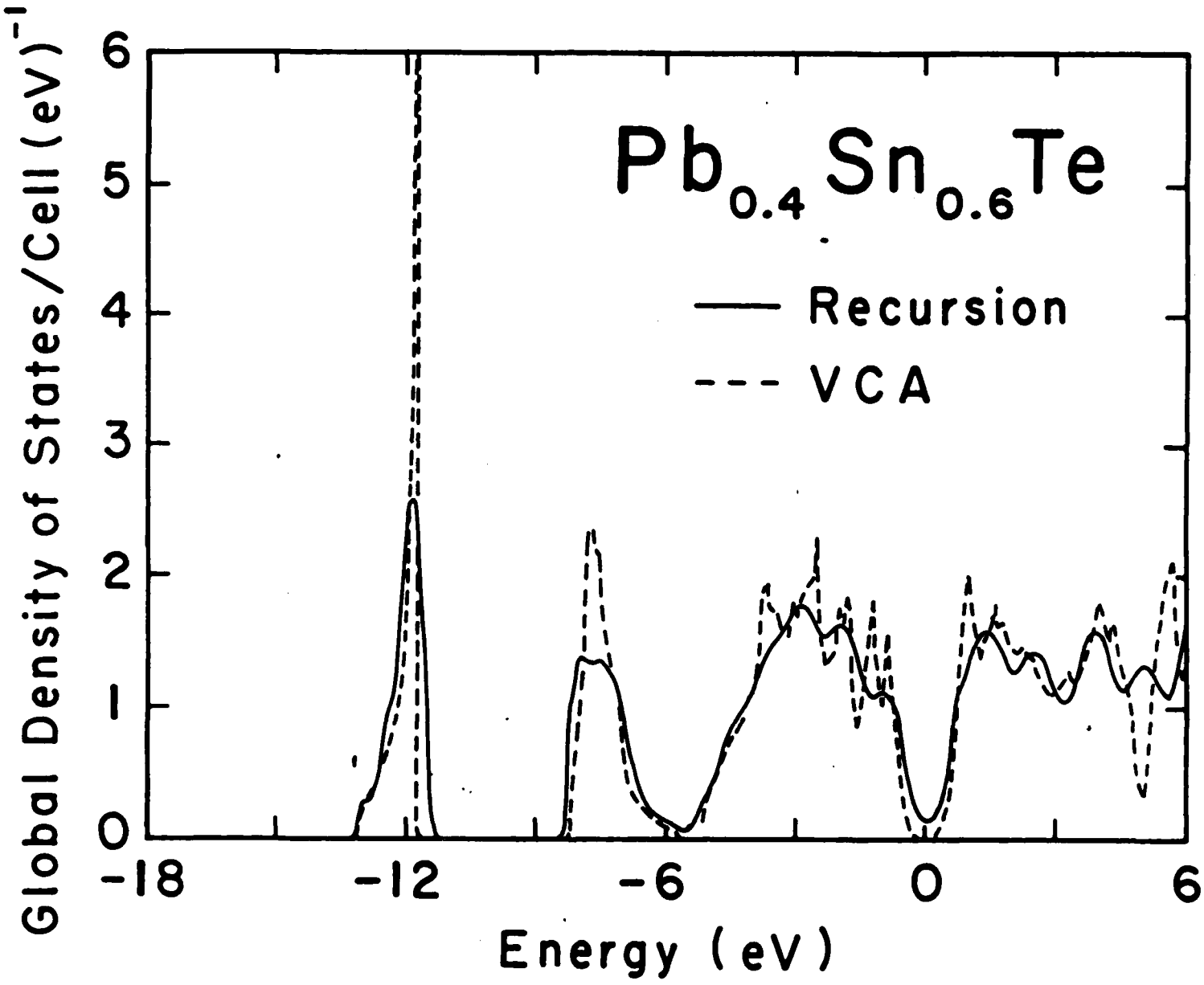
Pb0.4Sn0.6Te
Recursion
VCA
Global Density of States/Cell (eV)-1
Energy (eV)
0
1
2
3
4
5
6
-18
-12
-6
0
6

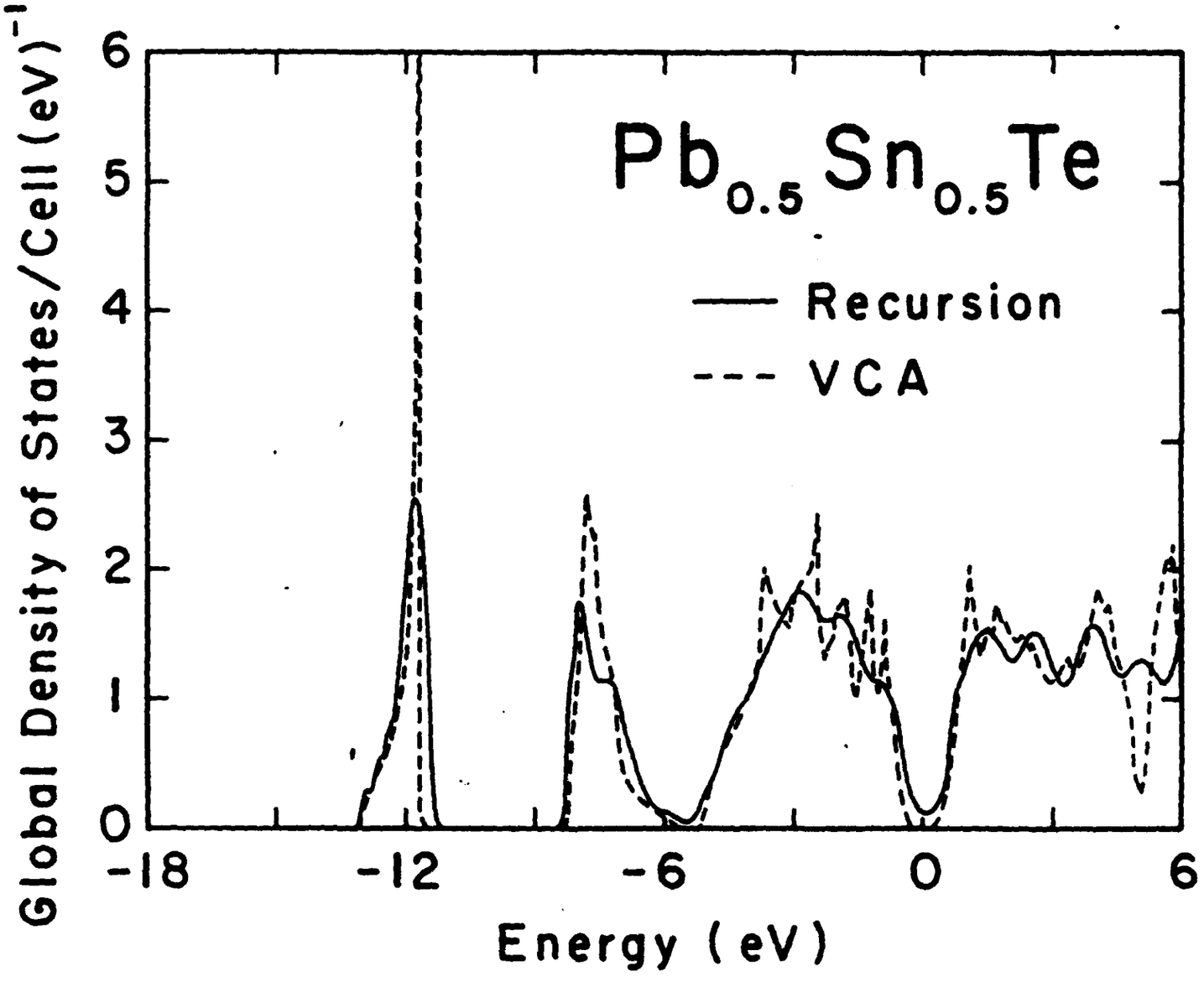
Global Density of States/Cell (eV)$^{-1}$
$Pb_{0.5}Sn_{0.5}Te$
Recursion
VCA
0
1
2
3
4
5
6
-18
-12
-6
0
6
Energy (eV)

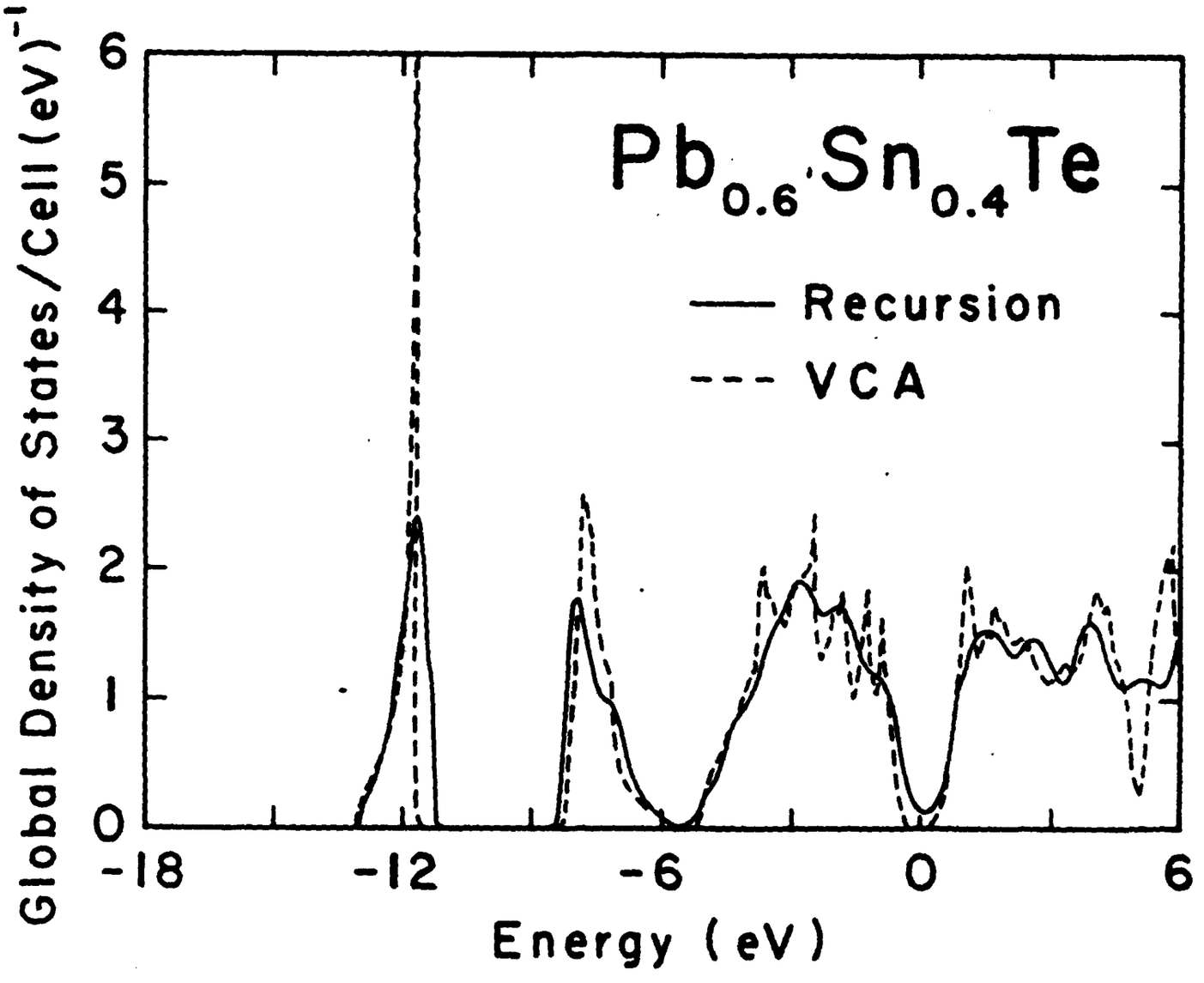
Global Density of States/Cell (eV)$^{-1}$
$Pb_{0.6}Sn_{0.4}Te$
Recursion
VCA
0
1
2
3
4
5
6
-18
-12
-6
0
6
Energy (eV)

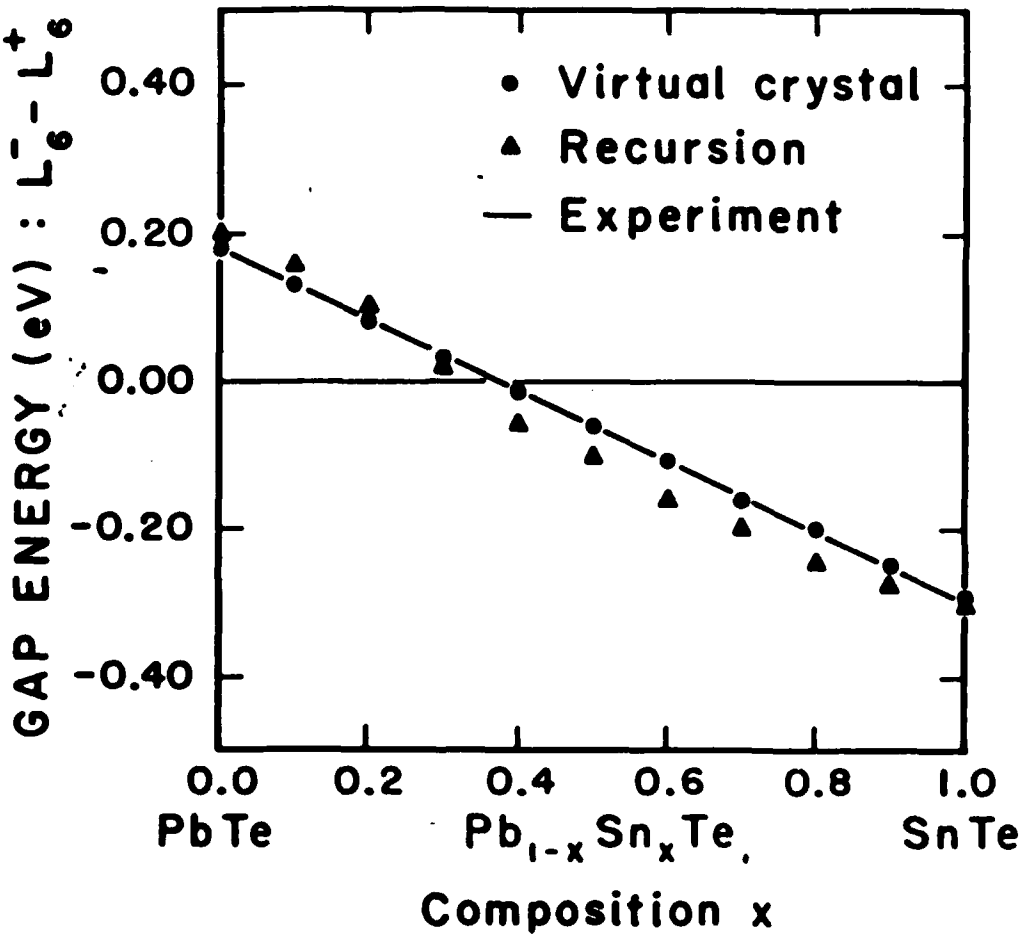
GAP ENERGY (eV) : $L_6^- - L_6^+$
0.40
0.20
0.00
-0.20
-0.40
Virtual crystal
Recursion
Experiment
0.0
0.2
0.4
0.6
0.8
1.0
PbTe
$Pb_{1-x}Sn_xTe$
SnTe
Composition x

file[dow.manus]fu211.rno 26 April 1987 21:46:50

"Clustering modes" in the vibrational spectra of $Hg_{1-x}Cd_xTe$ alloys

Zhuo-Wu Fu and John D. Dow

Department of Physics, University of Notre Dame

Notre Dame, Indiana 46556 U.S.A.

Abstract

The spectral densities of states for phonons in $Hg_{1-x}Cd_xTe$ alloys are predicted using the recursion method and are compared with Raman scattering data. The "clustering mode" observed by Amirtharaj et al. is shown to be an "alloy mode" associated with vibrations of a Te atom bonded to one Cd atom and three Hg atoms. $Hg_{1-x}Cd_xTe$ is shown to be a "two-mode" alloy vibrationally.

Recent Raman scattering data [1] for $Hg_{0.8}Cd_{0.2}Te$ substitutional crystalline alloys revealed a vibrational mode at 135 cm^{-1} that is neither Hg-like nor Cd-like. This "clustering mode" was thought to be caused by either non-random clusters in the alloy or by vacancies or vacancy-complexes. Motivated by these data, we have executed calculations of the densities of vibrational states of $Hg_{1-x}Cd_xTe$ random substitutional alloys, using the recursion method [2]. As a result: (i) We have determined that the "clustering mode" [1] is attributable to clusters of one Cd atom and three Hg atoms bonded to the same Te; there is no need to invoke vacancies or non-random clusters to describe the observed mode; and (ii) We have found that $Hg_{1-x}Cd_xTe$ is a "two-mode" alloy [3] in that the optical phonons of HgTe and CdTe persist for all x.

The calculations employ the recursion method [2], using a model with only short-ranged forces [4][5][6]. The method and model are essentially the same as those used for $Al_xGa_{1-x}As$ alloys [6] and $(GaAs)_{1-x}Ge_{2x}$ alloys [7], and so we do not repeat the formalism here. The recursion method is a Green's function theory, and, as such, has elements in common with the work of Talwar and Vandevyver [8]. The force constants used for HgTe and CdTe were fit to neutron-scattering data [9][10], and are given in Table I. They produce good phonon dispersion curves and vibrational densities of states [11][12].

Here we report the recursion calculations for $Hg_{0.8}Cd_{0.2}Te$, for which Raman scattering data are available [1]. Principal peaks of the spectra of HgTe and CdTe are identified in Fig. (1), using standard notation. In addition, "alloy modes," which appear in the spectra of neither HgTe nor CdTe, are indicated on Fig. (1). These modes are associated, in general, with

vibrations of specific clusters of atoms in $Hg_{1-x}Cd_xTe$. Such identifications of peaks in the spectra with particular clusters of atoms are obtained by choosing various specific mini-clusters [6][7] and by computing the local densities of states for one atom at the center of such a mini-cluster.

Comparing our theoretical results with the Raman scattering data of Amirtharaj et al. [1] (Fig. (1)), we find good agreement with the Cd-like optic mode at 156 cm^{-1} and the two Hg-like modes at 122 and 144 cm^{-1} respectively. The experimental "clustering mode" is simply an "alloy mode" [6] due to Te atoms bonded to three Hg atoms and one Cd atom. There is no need to invoke non-randomness in the alloy or to postulate the existence of vacancies in high concentrations.

We find that the optic modes of HgTe and CdTe persist for all alloy compositions x in $Hg_{1-x}Cd_xTe$. This is to be expected on the basis of the criterion of Onodera and Toyozawa [13]: because the masses of Hg and Cd are so different, the spectrum of $Hg_{1-x}Cd_xTe$ exhibits "two-mode" persistent behavior, and the optical phonon bands of HgTe and CdTe persist for all compositions x in the alloy $Hg_{1-x}Cd_xTe$. Note that the model on which the recursion calculations are based contains no long-ranged forces; hence the longitudinal and tranverse optic phonons are degenerate in this model at $\vec{k}=\vec{0}$, the Brillouin zone center. Since the experimental longitudinal-transverse optic phonon splitting at $\vec{k}=\vec{0}$ is small, the omission of the long-ranged Coulomb forces responsible for the splitting does not alter the essential physics or impede the identification of the principal spectral features.

In summary, recursion-method calculations of the densities of states of $Hg_{1-x}Cd_xTe$ alloys provide a natural identification of the "clustering mode" with vibrations of a complex involving three Hg atoms and one Cd atom bonded to the same Te atom. A complete discussion of phonons in these interesting alloys will be published soon [11].

Acknowledgments -- We are grateful to the U. S. Air Force Office of Scientific Research for their support (Contract No. AF-AFOSR-85-0331). We thank F. H. Pollack for calling our attention to this interesting problem.

REFERENCES

[1] P. M. Amirtharaj, K. K. Tiong, P. Parayanthal, F. H. Pollack, and J. K. Furdyna, J. Vac. Sci. Technol. A3, 226 (1985).

[2] R. Haydock, Solid State Physics, 35, ed. by H. Ehrenreich, F. Seitz, and D. Turnbull (Academic Press, New York, 1980), p. 215.

[3] G. Lucovsky, K. Y. Cheng, and G. L. Pearson, Phys. Rev. B 12, 4135 (1975).

[4] The model is the same as that of Ref. [5], except that the long-ranged forces are omitted, as in Ref. [6].

[5] R. Banerjee and Y. P. Varshni, Can. J. Phys. 47, 451 (1969).

[6] A. Kobayashi, J. D. Dow, and E. P. O'Reilly, Superlattices and Microstructures 1, 471 (1985).

[7] A. Kobayashi, K. E. Newman, and J. D. Dow, Phys. Rev. B32, 5312 (1985).

[8] D. N. Talwar and M. Vandevyver, J. Appl. Phys. 56, 1601 (1984).

[9] H. Kepa, W. Gebicki, T. Giebultowicz, B. Buras, and K. Clausen, Solid Stat. Commun. 34, 211 (1980).

[10] J. M. Rowe, R. M. Nicklow, D. L. Price and K. Zanio, Phys. Rev. B10, 671 (1974).

[11] Z.-W. Fu and J. D. Dow, to be published.

[12] The vibrational density of states is defined as follows: $\Sigma_{s,b,i} |\langle n,b,i|s\rangle|^2 \delta(\omega-\omega_s)$, where n labels the central unit cell of a 1000-atom cluster, b denotes either a (anion) or c (cation) in that cell, i runs over x, y, and z, and s labels the normal modes of the cluster: ω_s are the eigenfrequencies and $|s\rangle$ are the eigenvectors of the cluster. We used 51 levels of recursion, setting the fifty-first continued-fraction coefficient to

zero.

[13] Y. Onodera and Y. Toyozawa, J. Phys. Soc. Jpn. 24, 341 (1968).

TABLE

Table I. Force-constant parameters (in units of dyne/cm) and masses (in units of 10^{-24}g) for HgTe and CdTe, in the notation of Ref. [6].

	HgTe	CdTe
α	- 15875	- 19806
β	- 14635	- 18469
λ_c	5302	5304
λ_a	2579	1360
μ_c	- 2486	- 5281
μ_a	- 6650	- 2704
ν_c	- 4830	- 6954
ν_a	- 2930	2105
m_c	333.1	186.6
m_a	211.9	211.9

FIGURE CAPTIONS

Fig. (1). The Raman scattering data of $Hg_{1-x}Cd_xTe$, according to Ref. [1] (upper panel), in comparison with the calculated density of states of $Hg_{0.8}Cd_{0.2}Te$ (lower panel). The data were taken for the $<1\bar{1}0>$ face at 77K and are the curves 2a, 2e, and 2c (from the top down) of Fig. 2 from Ref. [1]. They correspond to the following experimental conditions: $X_2[Y_2,Y_2]\bar{X}_2$, $X_2[Z_2',Z_2']\bar{X}_2$, and $X_2[Y_2,Z_2]\bar{X}_2$, where we have $X_2[1\bar{1}0]$, $Y_2[110]$, $Z_2[001]$, and $Z_2'[\overline{112}]$. Principal spectral features are identified on the figure.

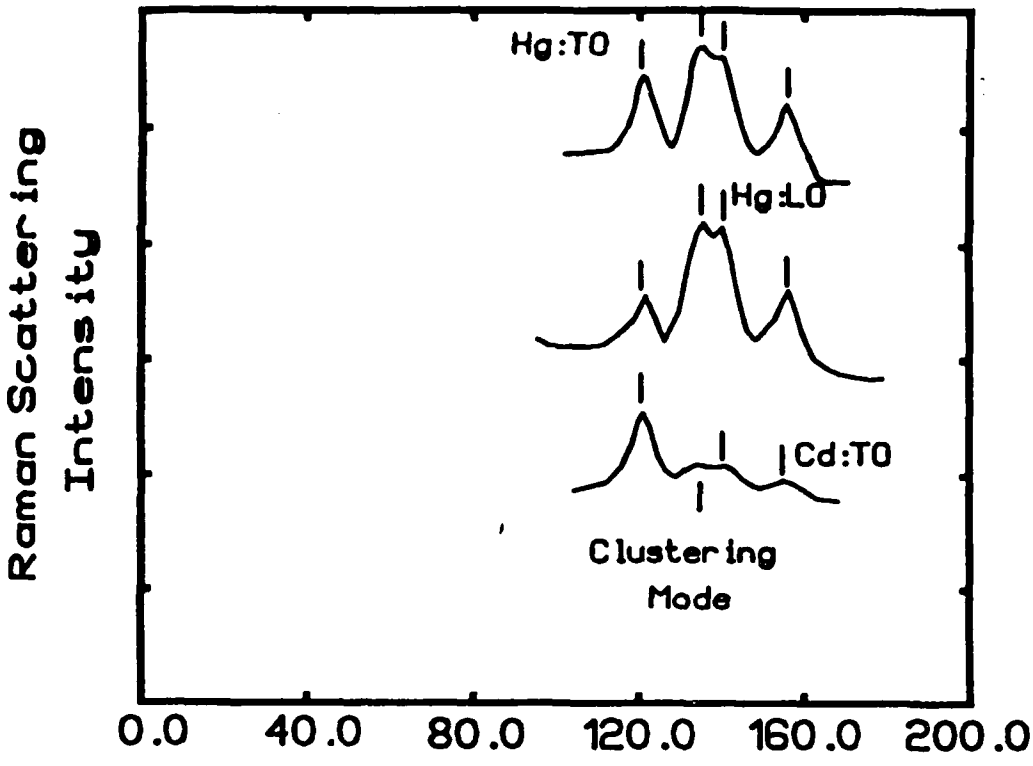
Raman Scattering Intensity
Hg:TO
Hg:LO
Cd:TO
Clustering Mode
0.0
40.0
80.0
120.0
160.0
200.0

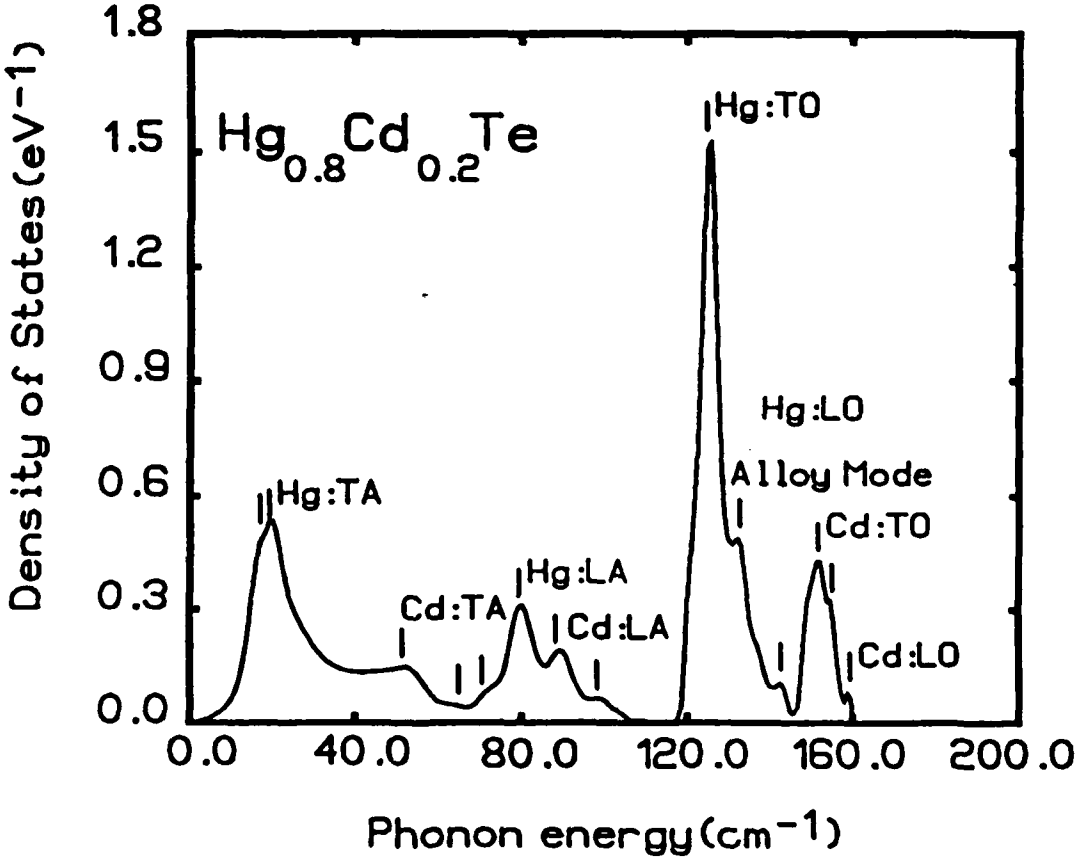
Density of States (eV-1)
1.8
1.5
1.2
0.9
0.6
0.3
0.0
Hg0.8Cd0.2Te
Hg:TO
Hg:LO
Alloy Mode
Cd:TO
Cd:LO
Hg:TA
Cd:TA
Hg:LA
Cd:LA
0.0
40.0
80.0
120.0
160.0
200.0
Phonon energy (cm-1)

OUR REFERENCE: file[dow.manus]ion202.rno 4 April 1987 16:07:18

Dependence on ionicity of the (110) surface relaxations of zincblende semiconductors

R. V. Kasowski

E. I. DuPont de Nemours and Company

Central Research and Development Department

Experimental Station, Wilmington, Delaware 19898

and

M.-H. Tsai and John D. Dow

Department of Physics, University of Notre Dame

Notre Dame, Indiana 46556

Abstract

It is argued that the surface relaxation angle ω of zincblende (110) surfaces should depend on ionicity or on longitudinal effective charge Z, approximately as $\omega = \omega_0 - \omega_1 Z^2e^2/\epsilon a_L$, with $\omega_1 \approx 6^o/eV$.

The (110) zincblende surface relaxations are thought to be the best understood of the semiconductor surface reconstructions, based on analyses of numerous low-energy electron diffraction (LEED) data [1][2][3][4][5][6][7][8][9][10] and medium-energy ion-blocking experiments [11][12]. It is widely believed that these reconstructions are determined virtually exclusively by covalent forces, and that the surface anions rotate more-or-less rigidly out of the surface through an angle $\omega \approx 29^{\circ}$ for all zincblende (110) surfaces [13][14][1][2]. (See Fig. 1.) This relaxation angle ω minimizes the energy of the covalent bonds. To be sure, some (110) zincblende surfaces have relaxations that are not purely rigid rotations of anions through 29°: (i) an opposite smaller rotation of the second layer followed by some inward relaxation of the top-bilayer toward the substrate [10] has been reported for some compound semiconductors [9][10][15]; and (ii) small variations in ω for different zincblendes have been purportedly correlated with variations of bulk lattice constants rather than ionicity (as previously proposed [16]) [18]. Nevertheless, the currently most-accepted viewpoint is that the (110) zincblende surface relaxations are remarkably well described by a rigid rotation model with a relaxation angle ω very near to 29° and virtually independent of ionicity.

However, the viewpoint that ω is constant for all zincblendes cannot possibly be precisely correct, and must be strictly valid only in the limit of low ionicity. For the more ionic zincblende semiconductors, the attractive Coulomb forces between the relaxed, negatively charged surface anions and the positively charged cations in and below the surface tend to pull the anions back toward the surface and reduce the relaxation caused by the covalent forces. (See Fig. 1.) This Coulombic effect should reduce the relaxation angle

ω by an amount proportional to Z^2, where Z is the (longitudinal) effective charge [19], and the effect should become significant when $Z^2e^2/\epsilon a_L$ is of order 0.5 eV, a typical covalent energy gained by each relaxing surface anion [20]. Here e is the electron's charge, ϵ is the dielectric constant, and a_L is the lattice constant. Recall that the ionicity f_i is approximately proportional to Z: $Z/Z_c \approx f_i$, where Z_c is the chemical valency [19].

Thus it is disturbing that LEED analyses of some zincblende semiconductors with quite different ionicities have yielded essentially the same values of ω [3][4][6], especially when one recognizes that the electronic properties of these surfaces depend dramatically on ionicity [21]. Clearly the surface physics of zincblende materials would advance if either (i) there were a convincing theoretical demonstration that ω should not depend significantly on ionicity, or (ii) there were revisions of the experimental values of ω that demonstrated a variation of ω with ionicity or effective charge Z.

To determine theoretically if the relaxation angles ω should indeed be the same for all zincblende semiconductors, we have executed self-consistent total-energy calculations based on the pseudo-function local-density theory [22]. These calculations employed four-atom-thick slabs of GaAs, InP, ZnTe, and ZnS [23], and allowed their (110) surfaces to relax via rigid rotations through angles ω until the total energies of the slabs reached minima. The resulting equilibrium relaxation angles ω are plotted in Fig. 2 as functions of $Z^2e^2/\epsilon a_L$ (See Table I.), and, to a good approximation, form a straight line described by the empirical rule

$$\omega = \omega_0 - \omega_1 Z^2e^2/\epsilon a_L,$$

with $\omega_0 = 20.62^\circ$ and $\omega_1 = 6.08^\circ/eV$. The fact that ω_0 is of the same general magnitude as the observed surface relaxation angles indicates that the rigid rotation model, as used here, contains the essential physics of the surface relaxation. We note also that the values ω we find for GaAs and other zincblendes are comparable with other theoretical values [9][17][24][20][25]. Furthermore, the sign and magnitude of ω_1 are as expected. While our computed relaxation angles do vary systematically with effective charge or ionicity, they show no such trend with lattice constant exclusively (See Table I) and therefore cast doubt on data analyses claiming to have determined such a correlations [18].

The relaxation angles ω extracted from data analyses are difficult to obtain accurately [10] (See Table I.), and actually agree about equally well with either hypothesis; (1) the widely believed $\omega \approx$ constant or (2) $\omega \approx \omega_0 - \omega_1 Z^2e^2/\epsilon a_L$, with ω_1 of order $6^\circ/eV$. (See Fig. 2.) Therefore we think that the $\omega \approx$ constant hypothesis should be reexamined experimentally, possibly by studying the (110) surfaces of zincblende CuCl, ZnS, CuI, and ZnSe (or some other highly ionic zincblende materials) in the light of the present results.

The ionicity of the zincblende surface not only reduces the equilibrium relaxation angle ω, but it also increases the relaxation energy per surface atom and increases surface phonon frequencies, according to the theory. (See Fig. 3.)

We hope that experiments on the (110) surfaces of different zincblende semiconductors will confirm these theoretical ideas quantitatively, establish the role of effective charge and ionicity in determining equilibrium surface geometry, and lead to an even better understanding of these prototypical

surfaces.

Acknowledgments -- We gratefully acknowledge enlightening conversations with Richard Martin about effective charges, and the support of the Air Force Office of Scientific Research (Contract No. AF-ASFOSR-85-0331). We also thank the E. I. du Pont Company for the use of their computational facilities, as well as partial support of M.-H. Tsai.

REFERENCES

[1] M. W. Puga, G. Xu, and S. Y. Tong, Surf. Sci. 164, L789 (1985).

[2] J. J. Barton, W. A. Goddard III, and T. C. McGill, J. Vac. Sci. Technol. 16, 1173 (1979); R. E. Allen, H. P. Hjalmarson, and J. D. Dow, Surf. Sci. 110, L625 (1981).

[3] C. B. Duke, A. Paton, and A. Kahn, J. Vac. Sci. Technol. A2, 515 (1984).

[4] C. B. Duke, A. Paton, A. Kahn, and D.-W. Tu, J. Vac. Sci. Technol. B 2, 366 (1984).

[5] C. B. Duke, A. Paton, and A. Kahn, J. Vac. Sci. Technol. A1, 672 (1983).

[6] C. B. Duke, A. Paton, A. Kahn, and C. R. Bonapace, Phys. Rev. B28, 852 (1983).

[7] C. B. Duke, A. Paton, A. Kahn, and C. R. Bonapace, Phys. Rev. B27, 6189 (1983).

[8] C. B. Duke, R. J. Meyer, and P. Mark, J. Vac. Sci. Technol. 17, 971 (1980).

[9] C. B. Duke, C. Mailhiot, A. Paton, D. J. Chadi, and A. Kahn, J. Vac. Sci. Technol. B3, 1087 (1985).

[10] P. G. Cowell, M. Prutton, and S. P. Tear, Surf. Sci. 177, L915, (1986).

[11] L. Smit, T. E. Derry, and J. F. Van Der Veen, Surf. Sci. 150, 245 (1985).

[12] L. Smit and J. F. Van Der Veen, Surf. Sci. 166, 183 (1986).

[13] S. Y. Tong, A. R. Lubinsky, B. J. Mrstik, and M. A. Van Hove, Phys. Rev. B 17, 3303 (1978).

[14] D. J. Chadi, Phys. Rev. B 18, 1800 (1978); 19, 2074 (1979).

[15] A. Kahn, Surf. Sci. 168, 1 (1986).

[16] S. Kurtin, C. A. Mead, and T. C. McGill, Phys. Rev. Lett. 22, 1433 (1969).

[17] C. Mailhiot, C. B. Duke, and Y. C. Chang, Phys. Rev. B30, 1109 (1984).

[18] See, e.g., C. B. Duke, J. Vac. Sci. Technol. B1, 732 (1983).

[19] G. Lucovsky, R. M. Martin, and E. Burstein, Phys. Rev. B 4, 1367 (1971).

[20] See Fig. 3 and, for example, K. C. Pandey, Phys. Rev. Letters 49, 223 (1982).

[21] R. S. Bauer, J. Vac. Sci. Technol. 14, 899 (1977).

[22] R. V. Kasowski, M.-H.Tsai, T. N. Rhodin, and D. D. Chambliss, Phys. Rev. B 34, 2656 (1986).

[23] The calculations for each material require about 150 hours of central processor time on an FPS-164 array processor.

[24] C. Mailhiot, C. B. Duke, and D. J. Chadi, Surf. Sci. 149, 366 (1985). These authors find relaxation angles ω of 27.8°, 28.9°, 29.5°, 30.9°, 31.5°, and 29.8° for GaP, GaAs, GaSb, InP, InAs, ans InSB, respectively.

[25] R. Chang and W. A. Goddard III, Surf. Sci. 144, 311 (1984). These authors find relaxation angles ω of 25.3°, 26.1°, 27.9°, 25.7°, 25.8°, 27.6°, 25.3°, 26.0°, and 27.9° for AlP, AlAs, AlSb, GaP, GaAs, GaSb, InP, InAs, and InSb, respectively.

[26] Ref. [24] is based on a phenomenological expression for the total energy as well as our tight-binding model (P. Vogl, H. P. Hjalmarson, and J. D. Dow, J. Phys. Chem. Solids 44, 365 (1983)) and therefore does not reproduce Coulomb effects properly. Ref. [25] is based on a six-atom cluster, and so the ions in the bulk that pull the surface anions back toward the bulk through the Coulomb force are not included in the model. Not surprisingly, both Ref. [24] and Ref. [25] find larger values of ω than we do.

Table I. Effective bulk (longitudinal) charges Z [19], lattice constants a_L (in units of Bohr radii a_0), dielectric constants ϵ [19], $Z^2e^2/\epsilon a_L$ (in eV), calculated relaxation angle ω_{Theory}, predicted change in relaxation angle $\Delta\omega$ (based on the empirical rule), and relaxation angles ω measured by low energy electron diffraction (ω_{LEED}) and ion back-scattering (ω_{ion}), respectively. See Ref. [19]. Note that our results for $_{Theory}$ are generally smaller than those of Ref. [24] and Ref. [25], especially for large effective charge Z, because of superior features of our model [26].

Materials	Z	$a_L(a_0)$	ϵ	$Z^2e^2/\epsilon a_L$	ω_{Theory}	$-\Delta\omega$	ω_{LEED}	ω_{ion}
CuCℓ	1.505	10.215	3.6	1.67		10.15°		
CuBr	1.35	10.753	4.4	1.048		6.37°		
CuI	1.715	11.419	5.2	1.347		8.19°		
AgI	1.38	12.232	4.9	0.864		5.25°		
ZnS	1.795	10.222	5.1	1.681	11°	10.22°	26° [3]	
ZnSe	1.625	10.710	5.9	1.137		6.91°	29° [4]	
ZnTe	1.66	11.529	7.3	0.891	14°	5.42°	28°±2° [5]	
CdTe	1.715	12.240	7.3	0.895		5.44°		
HgTe	2.025	12.208	14.0	0.653		3.97°		
BN	0.78*	6.831	4.5	0.538		3.27°		
AℓP	0.93*	10.301	7.6	0.301		1.83°	27.5°±3° [6]	
AℓAs	0.81*	10.700	9.0	0.185		1.12°		
AℓSb	1.045	11.594	10.2	0.251		1.53°		
GaP	1.185	10.300	8.5	0.436		2.65°	27.5° [3]	
GaAs	1.03	10.683	10.9	0.248	20°	1.51°	27°-31° [2]	29°±3° [11]
GaSb	0.69	11.519	14.4	0.078		0.47°	30°±2° [5]	28.5°±2.6° [12]
InP	1.485	11.090	9.6	0.563	17°	3.42°	28.1° [8]	
InAs	1.085	11.449	12.3	0.227		1.38°	31°±3° [7]	30°±2.4° [12]
InSb	0.72	12.243	15.6	0.074		0.45°	28.8° [8]	
SiC	0.775	8.217	6.7	0.297		1.81°		

* Estimated from the ionicity f_i by $Z = Z_c f_i$.

FIGURE CAPTIONS

Fig. 1. The rigid rotation model of the zincblende (110) surface geometry, as seen from the side, with the surface anions having relaxed through a relaxation angle $\omega = 29^{o}$. Note that the anions rotate up out of the surface, and that the bulk semiconductor lies in the lower part of the figure. Note also that the Coulomb forces between the negatively charged anions that have rotated out of the surface and the positively charged cations near and below them pull the surface anions back toward the surface.

Fig. 2. Calculated change $\Delta\omega = \omega - \omega_0$ of the relaxation angle ω as a function of $Z^2e^2/\epsilon a_L$ in eV. The calculations were performed for GaAs, InP, ZnTe, and ZnS (closed circles) and interpolated according to the empirical rule $\omega = \omega_0 - \omega_1 Z^2e^2/\epsilon a_L$ (open circles). Data for various semiconductors are plotted for comparison (See Table I.).

Fig. 3. Calculated total energy curves as a function of rotational relaxation angle ω for GaAs, ZnTe, and ZnS. Note that the effective charge Z increases from GaAs to ZnTe to ZnS. Note that the angle ω corresponding to equilibrium decreases with increasing ionicity or effective charge Z. (See Table I.) Note also that as the total energy curve becomes sharper and deeper, surface phonon frequencies increase.

Zincblende (110) surface

side view

$$\text{Force} \simeq -\frac{Z^2 e^2}{\varepsilon r^2}$$

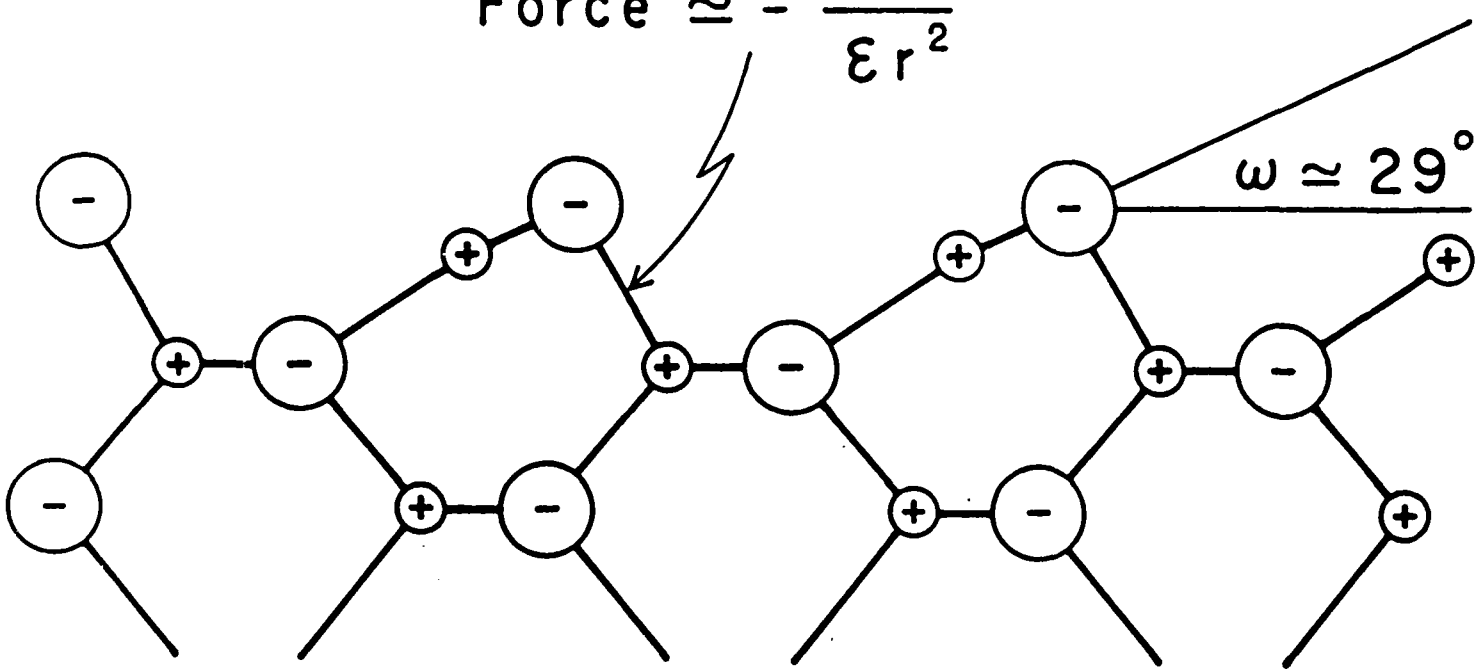

Coulomb force pulls surface anions down

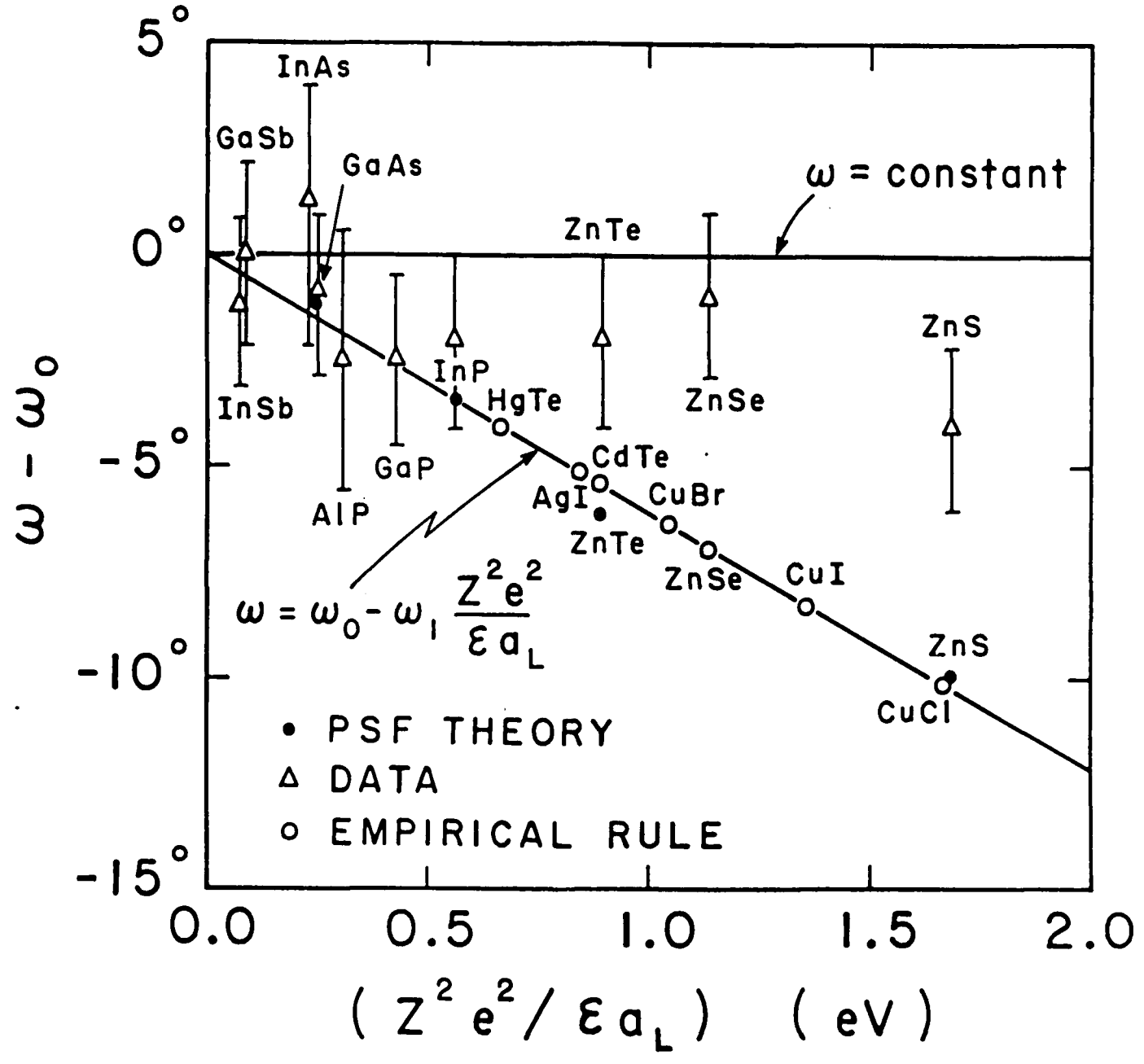
5°
0°
-5°
-10°
-15°
3 - 3°
InAs
GaSb
GaAs
ZnTe
ω = constant
ZnS
InP
InSb
HgTe
ZnSe
CdTe
GaP
AgI
CuBr
AlP
ZnTe
ZnSe
CuI
ZnS
CuCl
$\omega = \omega_0 - \omega_1 \frac{Z^2 e^2}{\varepsilon a_L}$
• PSF THEORY
△ DATA
○ EMPIRICAL RULE
0.0
0.5
1.0
1.5
2.0
$(Z^2 e^2 / \varepsilon a_L)$ (eV)

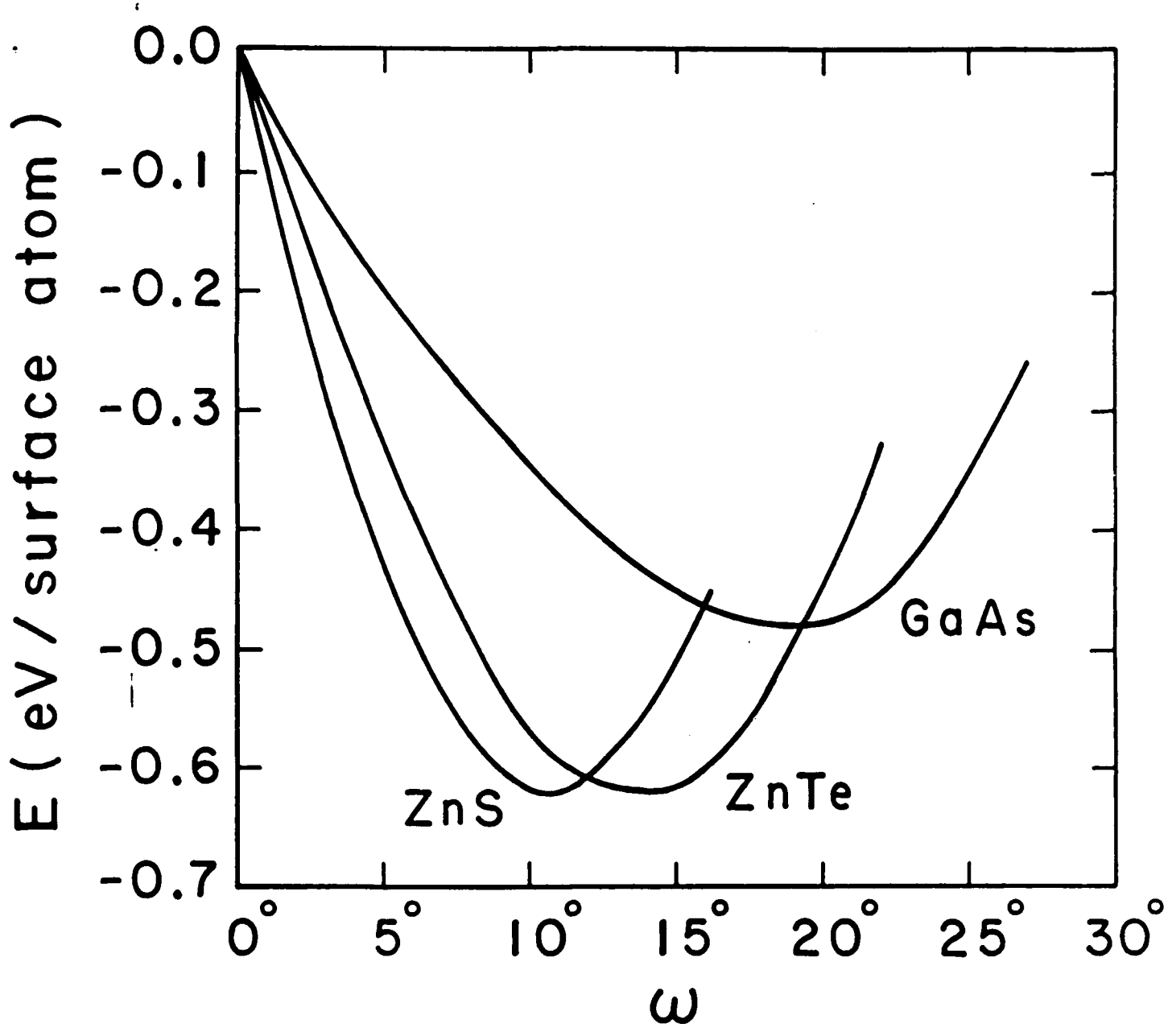
0.0
-0.1
-0.2
-0.3
-0.4
-0.5
-0.6
-0.7
E (eV / surface atom)
0°
5°
10°
15°
20°
25°
30°
ω
GaAs
ZnTe
ZnS

file[dow.manus]wur208.rno 10 April 1987 15:47:27

Reconstruction of the non-polar $(10\bar{1}0)$ surfaces of wurtzite AlN and ZnS

M.-H. Tsai

Department of Physics, University of Notre Dame

Notre Dame, Indiana 46556, U.S.A.

R. V. Kasowski

E. I. du Pont de Nemours and Company

Central Research and Development Department, Experimental Station

Wilmington, Delaware 19898, U.S.A.

and

John D. Dow

Department of Physics, University of Notre Dame

Notre Dame, Indiana 46556, U.S.A.*

and

Department of Chemical Engineering and Materials Science

University of Minnesota, Minneapolis, Minnesota 55455 U.S.A.

Abstract

Using the pseudo-function method and local density theory, we minimize the total energy of the $(10\bar{1}0)$ surfaces of AlN and ZnS, within the context of a Rigid Rotation Model. We predict that the surface anions rotate inward toward the bulk through very small angles (in contrast to the anions of the (110) surface of GaAs, which rotate outward through large angles ($\omega \simeq 29^{o}$). Thus, to an adequate approximation, the $(10\bar{1}0)$ surfaces of these relatively ionic wurtzite semiconductors do not reconstruct.

PACS Numbers: 68.20.+t; 73.20.-r

In this communication we present calculations of the surface relaxations of the non-polar $(10\bar{1}0)$ surfaces of wurtzite AlN and ZnS. We assume a Rigid Rotation Model of the surface similar to that developed for zincblende (110) surfaces by Tong and others [1][2], and calculate the angle of rotation ω that minimizes the surface's total energy.

Studies of zincblende (110) surfaces indicate that the primary chemistry determining their reconstruction is simple: surface anions that were four-fold co-ordinated in the bulk rotate out of the surface in order to re-hybridize their orbitals and adopt a three-fold co-ordination with bond angles that are near 90° and characteristic of three-fold co-ordinated molecules [3]. To an adequate approximation, bond-lengths are conserved during this rotational relaxation of zincblende (110) surfaces [4].

Guided by the success of the Rigid Rotation Model for the non-polar (110) surfaces of zincblende semiconductors, we propose an analogous model for the non-polar $(10\bar{1}0)$ surfaces of wurtzites, in which the reconstruction is described by a single angle ω, which gives the equilibrium rotation of the anions' surface-bonds, as described in Fig. (1). We then determine the equilibrium relaxation angle ω by minimizing the total energy, using local density theory [5] and the pseudo-function method [6]. To implement this procedure without using excessive computer time, we take the solid to be a slab four atoms thick, and, for simplicity, relax both the top and bottom layers symmetrically. Bond lengths are constrained to remain unaltered during this relaxation. (Such a procedure successfully described the physics of (110) zincblende relaxation [7].) Details of our calculational procedure may be found in Ref. [6].

In the minimum energy configuration, we find that the anions and cations of the $(10\bar{1}0)$ surfaces of wurtzite AlN and ZnS are very nearly on bulk lattice sites; the magnitudes of the equilibrium relaxation angles ω are <u>small</u> and <u>negative</u>, -2.5^{o} and -2.4^{o} for AlN and ZnS, respectively: the anions move slightly <u>inwards</u> toward the bulk (in contrast to the well-understood (110) zincblende surface, in which the anions relax out of the surface through a large angle of $\simeq 29^{o}$). The energies gained by this relaxation are 0.14 eV and 0.09 eV per surface atom for AlN and ZnS, respectively (much smaller that the 0.3 to 0.5 eV relaxation energies of zincblende (110) surfaces).

This resistance of wurtzite $(10\bar{1}0)$ surfaces to surface relaxation can be understood in terms of simple physics: Surface reconstruction is dictated by a competition between covalent forces and Coulomb forces. Atoms that are four-fold coordinated in the bulk are only three-fold co-ordinated at the surface, and covalent forces tend to rotate these atoms out of the surface through a relaxation angle ω into configurations such that they can re-hybridize and form three-fold co-ordinated bonds with bond-angles near 90^{o} (to accommodate the p_x, p_y, and p_z bonding orbitals [3]). The Coulomb forces, however, tend to counteract the covalent forces and pull the surface atoms back toward the bulk, because the nearest ion to a surface atom has an opposite charge to the surface atom. If the Coulomb forces are sufficiently strong in comparison with the covalent forces, the relaxation will be inhibited.

At zincblende (110) surfaces, relaxation energies are due primarily to covalent forces and are typically 0.3 to 0.5 eV (for large relaxation angles ω); moreover the zincblende relaxation angles are indeed large: on the (110)

surface of GaAs, the anions rotate by $\simeq 29^{o}$ up out of the surface so that their bond angles are nearly right angles [3][8]. Coulomb forces for a zincblende structure tend to pull the surface atoms down toward the bulk and are characterized by energies of order $Z^2e^2/\epsilon d$, where d is a surface bond length [9], Z is the longitudinal effective charge [10], e is the electron's charge, and ϵ is the dielectric constant [10]. For GaAs this Coulomb energy is small: 0.25eV [9]. Thus for the zincblende GaAs (110) surface, the covalent forces dominate the Coulomb forces and the anions rotate out of the surface through a large relaxation angle $\omega \simeq 29^{o}$ so that the bond angles of the anion are nearly 90^{o} [3].

For the $(10\bar{1}0)$ surfaces of wurtzite AlN and ZnS, the opposite is the case: Coulomb forces dominate the covalent forces. The corresponding [9] Coulomb energy for a wurtzite surface is $Z^2e^2/\epsilon a_L$, where a_L is the lattice constant, and is an order of magnitude larger than the Coulomb energy for zincblendes: 1.38 eV and 2.38 eV for AlAs and ZnS, respectively. This means that, at these wurtzite $(10\bar{1}0)$ surface, the Coulomb forces, not the covalent forces, should determine the reconstruction, and so the rotation angle ω should be considerably smaller than the 29^{o} characteristic of most zincblende (110) surfaces: to a reasonable approximation, these surfaces do not reconstruct. That is, we have ω near zero.

In a point-charge model, the Coulomb forces on the anions and cations in an unrelaxed $(10\bar{1}0)$ surface are the same and so do not, by themselves, lead to a rotation of the anions either into or out of the surface.

We attribute the slight inward rotation of the anions to the strong second-nearest-neighbor anion-anion interactions combined with Coulomb forces that are unbalanced at the surface: The anion-anion interactions (that is, the matrix elements of the crystal potential between orbitals centered on different anion sites) are strong and attractive, much stronger than the cation-cation interactions -- presumably because of the greater anion-anion covalent bonding. Furthermore, movement of the surface anions in toward the bulk as a result of these interactions shortens the distance from a surface anion to its two third-layer anions (See Fig. 1), further enhancing the anion-anion interactions. This third layer effect is larger than the effect on the inward anion movement of the four nearest-neighbor anions in the second layer, two whose distances to the surface anion are lengthened by the rotation, and two of whose distances are shortened -- layers, two whose distances to the surface anion are lengthened and cancelling out the effect in lowest order. In any event, the inward rotation is very small.

Thus, if we assume a Rigid Rotation Model of the wurtzite $(10\bar{1}0)$ surfaces of AlN and ZnS, we find that the relaxation angles ω are small and even negative. Since the model does not allow for small changes of bond length, which could be as important as small rotations of order $\omega \sim 2^{\circ}$, we cannot rule out the possibility that small bond length changes might quantitatively alter the relaxation angles. However we can conclude that, to an adequate approximation, the $(10\bar{1}0)$ surfaces of wurtzite AlN and ZnS do not reconstruct. Other wurtzite semiconductors with comparable ionicities and effective charges should also have $(10\bar{1}0)$ surfaces that are comparably well-described by a no-reconstruction model.

Finally we note that Duke et al. [11] have recently reported calculations of the ZnSe and ZnS $(10\bar{1}0)$ and $(11\bar{2}0)$ surfaces, and find results which are in conflict with ours: they find large positive bond rotation angles ω and considerable surface relaxation. We do not understand the physical origin of their results, and note that the physics we discuss here is not contained in the phenomenological model employed by Duke et al. That model replaces the Coulomb forces with a phenomenological contribution to the Hamiltonian which depends on bond-length changes. Such an approximation may not be valid at the surfaces of ionic compound semiconductors. We suspect that their model, by omitting the explicit Coulomb forces between the surface anions and the neighboring bulk atoms, also omits the force that inhibits the relaxation. As a result, their surface anions rotate unimpeded until they form bond angles near 90° -- and achieve a large relaxation angle ω. If our suspicion is correct, the addition of explicit Coulomb forces to their model should lead to small values of ω.

It will be an interesting challenge to the experimental surface physics community to determine which, if either, prediction is correct. Are the $(10\bar{1}0)$ surface relaxations of wurtzite AlN and ZnS large or small?

Acknowledgments -- We are grateful to the U. S. Air Force Office of Scientific Research (Contract No. AF-AFOSR-85-0331) and E. I. du Pont de Nemours and Company for their support.

REFERENCES

* Permanent address.

[1] S. Y. Tong, A. R. Lubinsky, B. J. Mrstik, and M. A. Van Hove, Phys. Rev. B 17, 3303 (1978).

[2] D. J. Chadi, Phys. Rev. B 18, 18000 (1978); 19, 2074 (1979).

[3] J. J. Barton, W. A. Goddard III, and T. C. McGill, J. Vac. Sci. Technol. 16, 1173 (1979).

[4] P. G. Cowell, M. Prutton, and S. P. Tear, Surf. Sci. 177, L915, (1986); A. Kahn, Surf. Sci. 168, 1 (1986); C. B. Duke, C. Mailhiot, A. Paton, D. J. Chadi, and A. Kahn, J. Vac. Sci. Technol. B3, 1087 (1985).

[5] L. Hedin and B. I. Lundqvist, J. Phys. C 4, 2064 (1971).

[6] R. V. Kasowski, M.-H. Tsai, T. N. Rhodin, and D. D. Chambliss, Phys. Rev. B34, 2656 (1986).

[7] R. V. Kasowski, M.-H. Tsai, and J. D. Dow, to be published.

[8] M. W. Puga, G. Xu, and S. Y. Tong, Surf. Sci. 164, L789 (1985).

[9] In terms of the zincblende latticeice constant a_L, we have $d = a_L/\sqrt{2}$.

[10] G. Lucovsky, R. M. Martin, and E. Burstein, Phys. Rev B4, 1367 (1971).

[11] C. B. Duke, Y. R. Wang, and C. Mailhiot, Bull. Amer. Phys. Soc. 32, 709 (1987). See also, C. Mailhiot, C. B. Duke, and D. J. Chadi, Surf. Sci. 149, 366 (1985).

Figure Caption

Fig. (1). Illustration of the reconstruction of the $(10\bar{1}0)$ wurtzite surface for a large positive relaxation angle ω. The anions and cations are denoted by - and + signs, respectively.

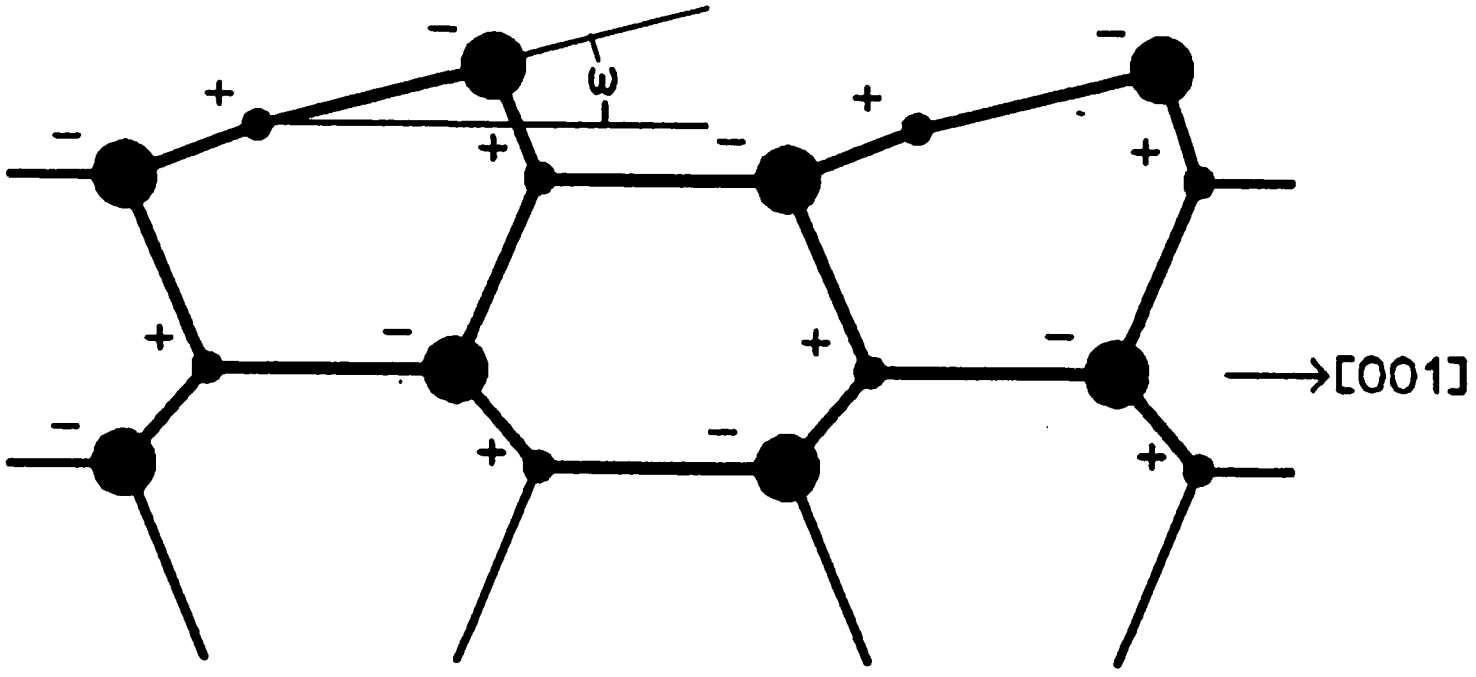

Side view of the wurtzite $(10\bar{1}0)$ surface

END

7-87

DTIC